The Astrophysical Journal, 992:197 (22pp), 2025 October 20 https://doi.org/10.3847/1538-4357/ae01a4

Signals of Bursts from the Very Early Universe

Leo Stodolsky[1] and Joseph Silk[2,3,4]
[1] Max-Planck-Institut für Physik, Boltzmannstr. 8, 85748 Garching, Germany
[2] Institut d'Astrophysique de Paris, UMR7095:CNRS UPMC-Sorbonne University, F-75014 Paris, France
[3] Department of Physics and Astronomy, The Johns Hopkins University, 3400 N. Charles St., Baltimore, MD 21218, USA
[4] BIPAC, University of Oxford, 1 Keble Rd., Oxford OX1 3RH, UK
Received 2024 November 2; revised 2025 August 27; accepted 2025 August 28; published 2025 October 15

Abstract

We consider possible observable signals from explosive events in the very early Universe, dubbed "bursts." These could be expected in connection with massive black hole or "baby Universe" formation. We anticipate that such major disruptions of spacetime would be associated with neutrino and perhaps other pulses. While these seem to be not detectable directly, we discuss how they could lead to potentially observable signals. We analyze how the pulses from very early times may "escape," that is, propagate to the last scattering epoch at the time $t_{\rm cmb}$ and later, or alternatively be absorbed earlier, i.e., "contained." The possibly detectable signals include effects on small regions of the cosmic microwave background, a soft X-ray resulting from positron production, or a nonthermal addition to the relic neutrino background.

Unified Astronomy Thesaurus concepts: Cosmic inflation (319)

1. Introduction

Some years ago (J. Silk & L. Stodolsky 2006), we contemplated the possibility that in the very early Universe, explosive events could take place, analogous to the supernovae seen in the presently observable Universe. These might be induced by such processes as the collapse of massive regions to black holes or the formation of "baby Universes." Although such events would lead to regions of spacetime which are physically disconnected from us, it is plausible that during their formation, peripheral or transient phenomena occur, as is familiar for the optical or neutrino bursts accompanying supernovae. Just as for the supernovae, a quiescent remnant may be left behind, while a dramatic explosive effect reaches the "outer world." Components of such bursts could reach us through their weakly interacting particles (L. Stodolsky 2000), and in J. Silk & L. Stodolsky (2006) we considered some of the basic features in terms of local observations on or near the Earth.

To set the context, the possibility of baby Universes was predicted from calculations of the wave function of the Universe (J. B. Hartle & S. W. Hawking 1983), and their actual formation was proposed by S. W. Hawking & R. Laflamme (1988). They are theoretically motivated by string theory, and more specifically by models such as eternal inflation (A. H. Guth 2000), and more recently by discussions such as R. Dijkgraaf et al. (2006) and A. Hebecker et al. (2018). Observational signatures have been studied of bubble Universe collisions, most notably via searching for hot spots in the cosmic microwave background (CMB) sky (S. M. Feeney et al. 2011). Bubble Universe creation is an ongoing phenomenon in the large number of scalar fields in the generic inflationary landscape (R. Easther et al. 2016).

Another formation channel for baby Universes is associated with the density fluctuation amplitude threshold for primordial black hole (PBH) formation (I. Musco et al. 2021). Exceed this and one produces baby Universes (B. J. Carr & S. W. Hawking 1974; M. Kopp et al. 2011). This idea couples the rate and abundance of baby Universe creation events to the PBH formation history and formation rate. This adds credibility to the baby Universe hypothesis, since PBHs provide a plausible scenario for dark matter with a number of potentially significant probes under development, most notably with next generation gravitational-wave observatories,

Observation or detection of such events would evidently open a new chapter in observational cosmology. However, there is a great difficulty in directly detecting the existence of such energetic but very early time events, namely the high redshift to be anticipated. The particles in the burst, such as neutrinos, will arrive at the Earth with an energy $a(t_{\rm em})E_{\rm em}$, where $E_{\rm em}$ is the energy in the rest frame of their emission, and $a(t_{\rm em})$ is the cosmological expansion parameter at the time of the burst. Thus neutrinos emitted from an event at cosmic time $t_{\rm em} = 1$ s will have their energies reduced by a factor (2×10^{-10}) at the Earth. Since the neutrino cross section for detection is strongly energy dependent, this would present formidable difficulties, even if we find (J. Silk & L. Stodolsky 2006) that the flux factor stops decreasing for very early emission times.

Here we would like to consider a less direct but perhaps more feasible approach toward finding evidence of such "early bursts," namely effects from the bursts at very early times or high redshift but nevertheless leading to a possibly observable signal.

We shall consider three possible such signals, involving different technologies. One would be the presence of positrons, created by burst neutrinos. These could give an observable soft X-ray signal (L. Stodolsky & J. Silk 2025).

Another is a "heat signal" concerning the energy injected by absorbed bursts into small regions on the CMB. We note that there is a rich literature on early energy injection into the CMB. This was pioneered by W. Hu & J. Silk (1993) and developed in many more recent studies, culminating in elegant theoretical formalisms including S. K. Acharya et al. (2023), in ground-breaking

experiments such as COBE-FIRAS (D. J. Fixsen et al. 1997), and in proposals for future CMB spectral distortion experiments (J. Chluba et al. 2021). Here we will use a simplified method, adapted to a qualitative discussion of the hypothesized bursts.

Finally, there is a question involving relic neutrinos. An important distinction concerning the bursts turns out to be if they can "escape," propagate to late times, or be "contained," absorbed at early times. The "escape" to present times of very low-energy neutrinos (or other weakly interacting particles) would lead to another, but very difficult to observe signal: a nonthermal component of relic neutrinos. This would involve new technologies for the observation of low-energy neutrinos (N. Rossi et al. 2024) and the determination of their spectrum.

This paper is at the interface of particle physics and astrophysics. We have chosen a style, frequently involving intuitive and approximate arguments, which we hope has enabled us to identify the important issues of this new subject. We trust this has made the discussion easily accessible to both communities.

2. Neutrino Propagation

The neutrino is the only known particle at present with purely weak interactions, and so it can travel relatively "far." In a core-collapse supernova almost all the energy is carried away by neutrinos. Although practically all types of particles are involved in the event and even the neutrinos themselves are in a transitory thermal equilibrium (the "neutrinosphere"), their weak interactions imply that they are the "first to leave" and carry most of the energy. We imagine that something analogous takes place in the case of "horizon collapse" and that the neutrinos carry most of the outgoing energy. However the energy spectrum of the individual neutrinos is a complicated matter, and we simply examine some illustrative models, hoping to extract some general features.

Behind the neutrino pulse, there can be more strongly interacting components, with electromagnetic or strong interactions. This would give rise to a localized heating, whose effects can also contribute to a "heat signal" discussed below.

2.1. Neutrino Mean Free Path

The distance traveled by a neutrino before it interacts is obtained from the mean free path λ, which is given by $\lambda = 1/(\rho\sigma)$, where ρ is the density of scatterers and σ is the cross section for the neutrino on the scatterer. We will take this to be a generic weak interaction cross section, whose most salient feature is its increase with energy. This leads to much greater containment for high-energy particles vis a vis low-energy ones (see Table 1).

The mean free path refers to a physical spatial distance and so should be used in conjunction with the proper distance. However in the standard cosmological spacetime metric that we use, $ds^2 = dt^2 - (a(t)\mathrm{dx})^2$, one has for essentially massless particles like neutrinos that $dt = a(t)dx$. Therefore when we write for the decay of a pulse $\sim -\lambda(t)dt$, we are in fact using the correct proper distance. Note that since we use $c = 1$ units (and generally natural units), λ is also the time between interactions for essentially massless particles.

The cross section will of course vary somewhat with the scatterer, but for our present semiquantitative purposes, we take a generic weak interaction cross section:

$$\sigma \approx \left(\frac{\alpha}{M^2}\right)^2 S, \tag{1}$$

with $\alpha = 1/137$, $M = 100\,\mathrm{GeV}$, and S is the center-of-mass energy squared of the scattering.

Equation (1) results from the exchange of W and Z bosons in the electro-weak standard model (W. Hollik 2022). The scatterers may be leptons, quarks or other particles interacting with neutrinos via such exchanges. A salient feature of Equation (1) is its energy dependence, which as will be seen below, leads to strong temperature and energy dependence of various aspects of the problem.

If $E^{\nu}(t)$ is the energy of the neutrino and $E^{i}(t)$ the energy of a scatterer, one has, averaged over directions, $S \approx E^{\nu}(t)E^{i}(t)$. This follows from $S = (p^{\nu} - p^{i})^2$ where the p are the four-momenta of a scattering partner i and the neutrino. This leads to the four-product $S \approx 2p^{\nu} \cdot p^{i} = 2E^{\nu}E^{i}(1 - \cos\theta)$, with θ the angle between the neutrino and the scattering partner i. After an angular average the $\cos\theta$ term drops out and one has $S \approx E^{\nu}(t)E^{i}(t)$ where, as throughout, we work only to order-of-magnitude accuracy.

At temperature T with the energy for a scattering partner $\sim T$ one will have $S \sim E^{\nu}(t)T(t)$. For the number density of particles ρ that one has for relativistic radiation

$$\rho \approx T^3, \tag{2}$$

and one thus arrives at

$$\lambda \sim \frac{M^4}{E^{\nu}T^4\alpha^2}, \tag{3}$$

where E^{ν} and T are time-dependent quantities, namely $T(t) = T_{\mathrm{now}}/a(t)$ and $E^{\nu}(t) = E^{\nu}_{\mathrm{em}}\frac{a(t_{\mathrm{em}})}{a(t)}$, where E^{ν}_{em} is the energy of a neutrino at emission.

Thus after emission, the neutrino has a mean free path $\lambda \sim a^5 \sim t^{5/2}$:

$$\lambda(t) = K \times (t/t_{\mathrm{rad}})^{5/2}, \tag{4}$$

where t_{rad} is a constant chosen so as to give the appropriate value to a in the radiation-dominated epoch (see Appendix). One then has the length or time constant

$$\begin{aligned} K &\approx \frac{1}{\alpha^2}\frac{M^4}{T^4_{\mathrm{now}}}\frac{1}{(E^{\nu}_{\mathrm{em}}/\mathrm{GeV})a(t_{\mathrm{em}})}\,\mathrm{GeV}^{-1} \\ &\approx (3 \times 10^{38})\,\frac{1}{a(t_{\mathrm{em}})(E^{\nu}_{\mathrm{em}}/\mathrm{GeV})}\,\mathrm{s} \\ &\approx (1 \times 10^{48})\,\frac{1}{(t_{\mathrm{em}}/\,\mathrm{s})^{1/2}(E^{\nu}_{\mathrm{em}}/\mathrm{GeV})}\,\mathrm{s}, \end{aligned} \tag{5}$$

with $E^{\nu}_{\mathrm{em}}/\mathrm{GeV}$ equal to the energy of a neutrino at emission in GeV units, and $T_{\mathrm{now}} = (2.5 \times 10^{-4})$ eV is the present temperature of the CMB. The probability of the neutrinos from a burst emitted at t_{em} reaching a time t without interacting is thus

$$\begin{aligned} \mathrm{Prob}(t, t_{\mathrm{em}}) \approx \exp\left[-\int_{t_{\mathrm{em}}}^{t}\frac{1}{\lambda}dt\right] = \exp\Bigg[-\frac{2}{3}\frac{t_{\mathrm{rad}}}{\mathrm{K}} \\ \times\,((t_{\mathrm{rad}}/t_{\mathrm{em}})^{3/2} - (t_{\mathrm{rad}}/t)^{3/2})\Bigg]. \end{aligned} \tag{6}$$

Table 1
Some Parameters for the Neutrinos Given Various Emission Times and Energies at Emission, Using Our Simplified Model

t_{em} (s)	z	E^{ν}_{em} (GeV)	E^{ν}_{cmb} (GeV)	t_{free} (s)	Prob_{∞}
10^{13}	10^{3}	10^{14}	1.0×10^{14}	3.6×10^{13}	1.1×10^{-3}
5×10^{12}	6×10^{3}	10^{13}	7.4×10^{12}	6.3×10^{12}	0.24
10^{12}	4×10^{3}	10^{17}	3.3×10^{16}	1.7×10^{15}	0.0
10^{12}	4×10^{3}	1×10^{3}	3.3×10^{2}	7.9×10^{5}	1.0
10^{12}	4×10^{3}	1×10^{10}	3.3×10^{9}	3.7	1.0
10^{10}	4×10^{4}	10^{6}	3.3×10^{4}	7.9×10^{3}	1.0
9×10^{8}	10^{5}	1	9.9×10^{-3}	7.6×10^{2}	1.0
9×10^{4}	10^{7}	100	9.9×10^{-3}	7.6×10^{2}	1.0
9×10^{2}	10^{8}	1000	9.9×10^{-3}	7.6×10^{2}	0.46
9	10^{9}	10^{4}	9.9×10^{-3}	7.6×10^{2}	0.0
1	4×10^{9}	10^{5}	3.3×10^{-2}	1.7×10^{3}	0.0
0.1	10^{10}	10^{5}	1.1×10^{-2}	7.9×10^{2}	0.0
0.1	10^{10}	10^{3}	1.1×10^{-4}	36	0.0
0.1	10^{10}	10^{1}	1.1×10^{-6}	3.7×10^{-1}	8.1×10^{-4}
0.1	10^{10}	10^{-1}	1.1×10^{-8}	7.9×10^{-2}	0.50
10^{-2}	4×10^{10}	10^{-1}	3.3×10^{-9}	3.7×10^{-2}	2.3×10^{-10}
10^{-2}	4×10^{10}	10^{-2}	3.3×10^{-10}	7.9×10^{-3}	0.50
10^{-4}	4×10^{11}	10^{-3}	3.3×10^{-12}	3.6×10^{-4}	1.1×10^{-3}
10^{-5}	10^{12}	10^{-4}	1.1×10^{-13}	3.6×10^{-5}	1.1×10^{-3}
10^{-5}	10^{12}	10^{-5}	1.1×10^{-14}	7.9×10^{-6}	0.50
10^{-6}	4×10^{12}	10^{-6}	3.3×10^{-16}	7.9×10^{-7}	0.50
10^{-9}	10^{14}	10^{-8}	1.1×10^{-19}	3.7×10^{-9}	8.1×10^{-4}
10^{-10}	4×10^{14}	10^{-8}	3.3×10^{-20}	1.7×10^{-9}	3.6×10^{-31}

Note. The second column, z, is the redshift corresponding to the emission time, and the third is the emission energy. The fourth column is the energy after the redshift to t_{cmb}, using $E^{\nu}_{cmb} = (3.3 \times 10^{-7})\,(t_{em}/\text{ s})^{1/2} E^{\nu}_{em}$, and the fifth column is t_{free}, as found from Equation (11). At an emission time of 0.1 s a neutrino with energy below 100 MeV can escape, while at 10^{-6} s, the energy must be below 1 keV. One notes that the probability of escape to large times P_{∞} becomes essentially zero when the emission time is before t_{free}. In these cases, with $P_{\infty} \approx 0$, t_{free} gives the time by which the neutrinos have interacted (see text).

With $t_{rad} = (1.9 \times 10^{19})$ s, the characteristic dimensionless parameter t_{rad}/K in Equation (6) has the value, for say $t_{em} = 1$ s, $E^{\nu}_{em} = 1$ GeV, of $\sim(1 \times 10^{-29})$.

It is to be noted that in Equation (6) the time t appears in the exponent inversely and to a fractional power. This is quite different from usual "optical depth" expressions, where it appears linearly. This difference originates in the time dependence of the medium and the energy dependence of the neutrino cross section.

2.2. The Parameter t_{free}

The analysis becomes more transparent if we introduce a time t_{free}, defined as

$$t_{free} = \left(\frac{2t_{rad}}{3\text{ K}}\right)^{2/3} t_{rad}. \tag{7}$$

The interpretation of t_{free} is given at the end of this subsection. With this definition, Equation (6) becomes

$$\text{Prob}(t,\, t_{em}) = \exp\left[-(t_{free}/t_{em})^{3/2} + (t_{free}/t)^{3/2}\right], \tag{8}$$

which also can be written as

$$\begin{aligned}\text{Prob}(t,\, t_{em}) &= \exp\left[-(t_{free}/t_{em})^{3/2}\right] \\ &\quad \times \exp\left[+(t_{free}/t)^{3/2}\right] \\ &= \exp\left[-\kappa^{3/2}\right] \times \exp\left[+(t_{free}/t)^{3/2}\right],\end{aligned} \tag{9}$$

where we introduce the ratio κ

$$\kappa = t_{free}/t_{em}. \tag{10}$$

The time dependence is given by the second factor in Equation (9). Although this factor is a decreasing function, one notes that the expression does not tend to zero for $t \to \infty$. Rather it goes to one, not zero, for large t.

While Prob(t, $t_{\rm em}$) thus no longer decreases as $t \to \infty$, this can happen in two ways. The first factor, $\exp[-\kappa^{3/2}]$, can be of order one, or it can be very small, close to zero. When it is of order one, it means that the neutrinos have "escaped" to late times without interacting. When it is near zero it means that the neutrinos have not reached late times, they have been "contained." There are thus two regimes of behavior, according to whether one has $t_{\rm em} > t_{\rm free}$, that is, $\kappa < 1$; or $t_{\rm em} < t_{\rm free}$, that is, $\kappa > 1$.

Cases with $t_{em} > t_{free}$. The emission is later than $t_{\rm free}$. Since $t_{\rm free}/t < 1$ always, the exponent in the second factor of Equation (9) is always small and the factor varies little. This is the justification for the label "free," i.e., the neutrinos are moving freely. This "escape" reflects the fact that the dilution of the medium and the redshifting of the energy has dominated over the absorption of the neutrinos.

Cases with $t_{em} < t_{free}$. The emission takes place earlier than $t_{\rm free}$. Then the exponent of the second factor of Equation (9) is large and the factor decreases rapidly until the burst is totally absorbed. One sees that the period of rapid decrease ends when $t \approx t_{\rm free}$. Hence in these cases $t_{\rm free}$ is the time by which the neutrino pulse is absorbed.

The significance of $t_{\rm free}$ is thus that it determines if a neutrino "escapes" or not, and if it does not, the time by which it is "contained." As shown in Table 1, the transition around $\kappa \sim 1$ is rather abrupt and we can regard $\kappa = 1$ as a dividing line between the two regimes of "escape" or "containment."

2.3. Numerical Estimates

For the quantitative evaluation of $t_{\rm free}$, we write

$$\begin{aligned} t_{\rm free} &= \left(\frac{2t_{\rm rad}}{3{\rm K}}\right)^{2/3} t_{\rm rad} \\ &= \left(\frac{2\,(t_{\rm em}/\ {\rm s})^{1/2}(E^{\nu}_{\rm em}/{\rm GeV})t_{\rm rad}}{3\times(1\times 10^{48})}\right)^{2/3} t_{\rm rad} \\ &= (4\times 10^{-20})\,((t_{\rm em}/\ {\rm s})^{1/2}(E^{\nu}_{\rm em}/{\rm GeV}))^{2/3} t_{\rm rad} \\ &= (8\times 10^{-1})\,((t_{\rm em}/\ {\rm s})^{1/2}(E^{\nu}_{\rm em}/{\rm GeV}))^{2/3}\ {\rm s}. \end{aligned} \tag{11}$$

This result may also be written as

$$\kappa = \frac{t_{\rm free}}{t_{\rm em}} = (8\times 10^{-1})\left(\frac{E^{\nu}_{\rm em}/{\rm GeV}}{t_{\rm em}/\ {\rm s}}\right)^{2/3}. \tag{12}$$

From the form of Equation (12), one sees that a constant value of κ, which gives the "escape" probability, arises from a constant ratio between $E_{\rm em}$ and $t_{\rm em}$. In particular $\kappa = 1$ corresponds to the conditions

$$\begin{aligned} t_{em}/\ {\rm s} &= (7\times 10^{-1})\ E^{\nu}_{\rm em}/{\rm GeV}, \\ x_{\rm em} &= (8\times 10^{-14})\,E^{\nu}_{\rm em}/{\rm GeV}, \end{aligned} \tag{13}$$

where $x_{\rm em} = t_{\rm em}/t_{\rm cmb}$ refers to a dimensionless scaled time variable $x = t/t_{\rm cmb}$ that we shall use below. We shall refer to the parameter (8×10^{-14}) as "s" in the following:

$$s = (8\times 10^{-14}). \tag{14}$$

These numerical values arise from our simplified assumptions, which have allowed us to identify the qualitative features of the problem. While the numbers may be expected to change in more detailed treatment, the general features may be expected to remain, namely a division of the ($t_{\rm em}$, $E^{\nu}_{\rm em}$) space into an "escape" and a "confined" region, with an approximately linear, increasing, boundary between the two.

Table 1 shows some of the parameters for sample emission time and emission energy, using Equation (11). The first column is the emission time, the second is the corresponding redshift z, the third column is the energy of the neutrino, the fourth is the energy after the redshift to $t_{\rm cmb}$, and the fifth is $t_{\rm free}$. The last column is the quantity P_{∞}, the first factor in Equation (9), giving the probability of "escape" to large times:

$${\rm Prob}_{\infty} = \exp[-(t_{\rm free}/t_{\rm em})^{3/2}] = \exp[-\kappa^{3/2}]. \tag{15}$$

Since $t_{\rm cmb}$ will generally be much later than our other times, ${\rm Prob}_{\infty}$ will also be the probability that a neutrino reaches the formation time of the CMB or the time of the last scattering, $t_{\rm cmb}$. One sees how the probability of "escape" essentially depends on whether the emission is before or after $t_{\rm free}$.

2.4. The Time–E$_{em}$ Plane

Visualization is aided by a sketch of the time–$E_{\rm em}$ plane, shown in Figure 1. The figure shows the separation in this plane into regions for "contained" or "escaping" neutrinos. The time is represented by the vertical axis, but since we will be mainly concerned with neutrinos at $t_{\rm cmb}$, we use the dimensionless scaled time

$$x = t/t_{\rm cmb}. \tag{16}$$

The horizontal axis is the emission energy.

The $\kappa = 1$ line is shown ascending to the right, given by $x = sE_{\rm em}/{\rm GeV}$, as in the second form of Equation (13). This line separates the plane into regions of "escape" (above the line) and "contained" (below the line), according to whether κ is greater than or less than one.

It is also interesting to show where in the plane neutrinos which can arrive to $t_{\rm cmb}$ with a certain energy originate. The curves for a given $E^{\nu}_{\rm cmb}$ are sketched using the radiation-dominated $x = (E_{\rm cmb}/E_{\rm em})^2$ formula for redshift. Following a curve down from $x = 1$ to earlier times or smaller x, gives the points which potentially contribute to a given energy of the neutrino spectrum at $t_{\rm cmb}$. However if the curve goes below the $x = sE_{\rm em}/{\rm GeV}$ "escape" line, that region cannot contribute. Similarly if the emission spectrum does not extend beyond a certain $E_{\rm max}$, the region to the right of $E_{\rm max}$ is also excluded. A curve enters the forbidden region for "escape" at time $x = (sE_{\rm em}/{\rm GeV})^{2/3}$ and when there is an $E_{\rm max}$ constraint, at time $x = (E_{\rm cmb}/E_{\rm max})^2$.

An interesting conclusion from these "escape" considerations is that a very low-energy neutrino cannot originate from a very high-energy neutrino. The curve for a small $E^{\nu}_{\rm cmb}$ will generally enter the forbidden zone for "escape" before it gets to high energy. That is, the large redshift needed would imply emission at an early time, where it would however be stopped before reaching later times.

3. Morphology

A burst at time $t_{\rm em}$ will spread out from its point of origin. The furthest traveling component among the presently known elementary particles and probably its principal one, will be the neutrinos. Since these travel essentially at the speed of light, the radius they reach at $t_{\rm cmb}$ gives the outer radius of the region where possible signs of the bursts on the CMB will show. We

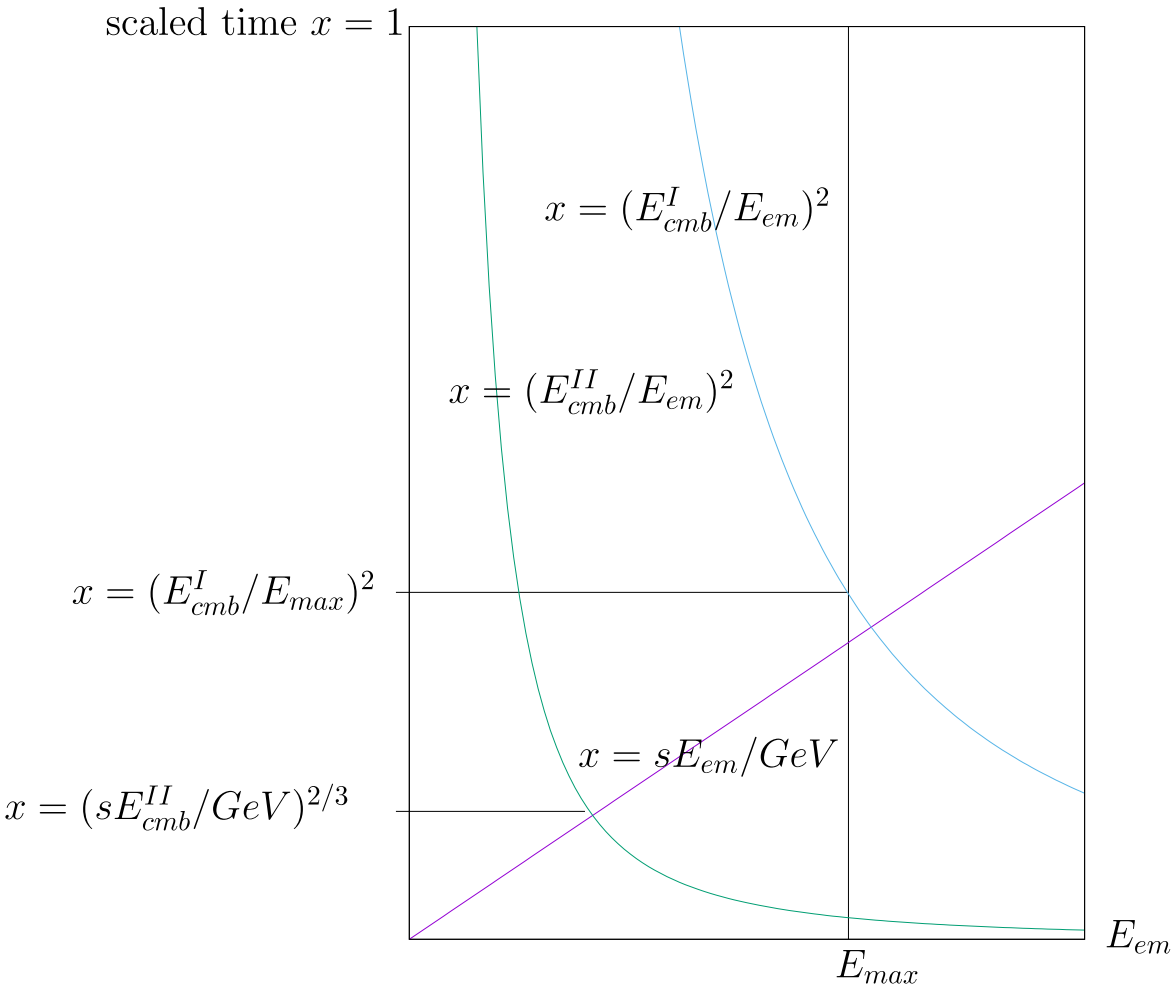

Figure 1. The emission energy–emission time plane for the free flight of neutrinos. $E_{\rm em}$ is the emission energy and x is the scaled emission time. The plot shows which regions can or cannot contribute to a given $E^{\nu}_{\rm cmb}$ at scaled time $x = 1$. The inclined line rising to the right, $x = sE_{\rm em}/{\rm GeV}$, separates the plane into the regions of "escape" (above the line) and "contained" (below the line). In the well-defined $\bar{E}^{\nu}$ model, the potentially contributing regions would correspond to a vertical band at some $E_{\rm em} = \bar{E}^{\nu}$ (not shown). For the spread spectrum model, where all energies up to a certain maximum $E_{\rm max}$ can occur, the region to the left of $E_{\rm max}$ potentially contributes. Points that can contribute to a given $E^{\nu}_{\rm cmb}$ are found by following a curve down from the point where it starts at $x = 1$. The two curves are examples for particles with different energies at $x = 1$. The curve to the right, Curve I, is for a relatively higher energy and the curve to the left, Curve II, is for a lower energy. Curve I encounters the $E_{\rm max}$ limitation before encountering the "escape" limitation. For Curve II it is the other way around. These two possibilities lead to the different lower limits of integration in Equation (61).

say "radius" under the assumption that the burst is spherical; if not our numerical results should be taken as merely qualitative.

We consider two situations, one where the neutrinos (or other weakly interacting, essentially massless, particles) "escape," that is travel freely to $t_{\rm cmb}$ and later, or alternatively where they are absorbed earlier. As explained above, this will be given by the parameter $t_{\rm free}$, see Section 2.2.

3.1. Neutrino Burst Radius: "Escape"

With the neutrinos traveling at the speed of light (small neutrino mass and index of refraction effects are negligible) the radius or linear dimension for free flight until $t_{\rm cmb}$ is given by

$$a(t_{\rm cmb})\int_{t_{\rm em}}^{t_{\rm cmb}}(1/a)dt = 2t_{\rm cmb}\left(1-\left(\frac{t_{\rm em}}{t_{\rm cmb}}\right)^{1/2}\right) \approx (2\times 10^{13})\ {\rm s} \quad \text{for } t_{\rm cmb} \gg t_{\rm em}. \tag{17}$$

For early bursts , this is independent of the emission time and corresponds to an angular dimension of 2×10^{-2} radians on the CMB. In our symbolic representation Figure 2, we represent these "escaped" bursts by the larger little circles, all of the same size.

3.2. Neutrino Burst Radius: "Contained"

When the neutrinos are "contained," then the burst energy reaches out to a minimum radius $t_{\rm free}$ by "free flight." That is, the neutrinos travel freely between the times $t_{\rm em}$ and $t_{\rm free}$. A further propagation of the burst might be relevant by a diffusion-like process of the particles produced by the neutrino interactions. These will be essentially particles with strong or electromagnetic interactions with a much shorter interaction length, resulting in a diffusive behavior. We give rough estimates of the lengths involved. These lengths are relevant both for understanding the possibly observable size of the resulting region on the CMB, and for estimating the volume in which the burst energy is deposited.

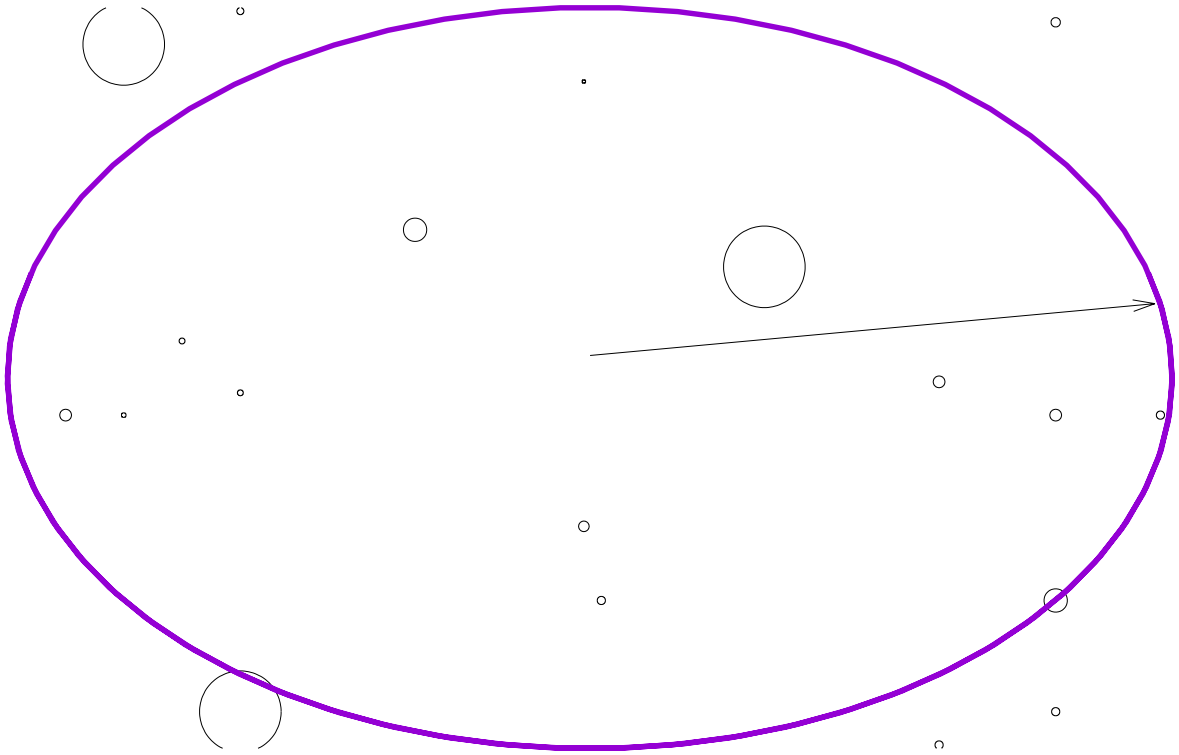

Figure 2. Symbolic, in only two spatial dimensions and not to scale, representation of how bursts would appear on the last scattering surface (LSS) at $t_{\rm cmb}$. The large thick circle stands for the intersection of our backward light cone (BLC) with the LSS. Its radius is indicated by the arrow and its thickness is meant to represent the finite size of the observable region. The radius increases by 10^{-3} lt-yr in 1 Earth year. The larger of the smaller circles represent"escaping" neutrinos, which reach $t_{\rm cmb}$ or later times. According to Equation (17), these are all of about the same size. The smallest circles represent "absorbed" bursts, whose radius is governed either by $t_{\rm free}$, or the "diffusion distance." Observations via photons are given symbolically by the intersection of the large circle with the burst areas. In 2D this is a line segment, but in the real 3D case the circles become spheres, so the intersection with the BLC becomes a disk. We have assumed that the bursts are spherically symmetric.

3.2.1. Free Flight

The "free flight" distance may be found as in Equation (17), with the difference that the coordinate distance is given by $t_{\rm free}$ and not $t_{\rm cmb}$. The $a(t)$ factor, however, is still $a(t_{\rm cmb})$ since we wish to obtain the proper size at $t_{\rm cmb}$. Thus for contained bursts the radius or linear dimension at $t_{\rm cmb}$ is

$$a(t_{\rm cmb})\int_{t_{\rm em}}^{t_{\rm free}}\frac{dt}{a} = 2t_{\rm cmb}^{1/2}(t_{\rm free}^{1/2}-t_{\rm em}^{1/2}) \approx (2\times 10^{13})\,(x_{\rm free}^{1/2}-x_{\rm em}^{1/2})\ {\rm s}, \qquad (18)$$

using the scaled time $x=\frac{t}{t_{\rm cmb}}$.

As Table 1 shows, large ranges of $x_{\rm free}$ and $x_{\rm em}$ are imaginable, so unless the bursts are concentrated around a certain emission time with a definite energy, a large range of radii are possible, up to $\sim(2\times 10^{13})$ s. On the other hand, should the bursts be mainly from a certain time $x_{\rm em}$, then Equation (18) could help to identify that time. In Figure 2 we represent these "contained" bursts by the smaller little circles. These are of varying size, in accordance with Equation (18).

3.2.2. Diffusion Length

A second mechanism for the spread of the burst is possible, namely diffusion-like processes. When the neutrinos interact, most of the energy will be transferred to an electromagnetic or hadronic component, in reactions of the type

$$\nu\rightarrow e^{-}....,\quad \nu\rightarrow \mu^{-}.... \qquad (19)$$

where ... can be hadrons, quarks, or other components of the electro-weak standard model. These components, having electromagnetic or strong interactions, will have a much shorter interaction length than neutrinos. We estimate a diffusion parameter based on their cross sections. The electromagnetic component is characterized by the cross section $\sigma\sim\alpha^2/m_e^2$ and the strong interaction component by $\sigma\sim 1/(100\,{\rm MeV})^2$. Both of these are roughly energy independent and have about the same size, so we treat them together. This separation into weak and other components is a simplification since there will be transfers between the components, but after the neutrinos interact most of pulse will consist of the non–weakly interacting components.

Diffusion may be viewed as a random walk process, and to find a diffusion length, we use a random walk argument with the above electromagnetic/strong interaction parameters.

Because we have a small, isolated system we are able to treat the problem in a simple way, without general relativistic considerations and particular coordinate systems. We use the equivalence principle, which says that in a small "freely falling" system the gravitational field is eliminated (L. D. Landau & E. M. Lifshitz 1962). We thus place ourselves in the rest frame around the origin of the burst. There is no gravitational field and the problem then becomes one of a random walk in a medium of decreasing density. The length found is then automatically a proper length. In such problems, one finds the variance Var in the probabilistic location of the particle, given by the number of

collisions. The square root of the variance then gives the characteristic length.

The size of the step in the random walk here is given by the distance between collisions or the mean free path. Using $\sigma \sim 1/(100\,\mathrm{MeV})^2$ from $\lambda = 1/(\rho\sigma)$ one has

$$\lambda = \frac{(100\,\mathrm{MeV})^2}{T^3} = \frac{(100\,\mathrm{MeV})^2}{T_{\mathrm{now}}^3}(t/t_{\mathrm{rad}})^{3/2} = (4 \times 10^{11})\,(t/t_{\mathrm{rad}})^{3/2}\,\mathrm{s}. \quad (20)$$

At $t = 1$ s, for example, one has $\lambda \sim (6 \times 10^{-18})$ s, and around t_{cmb} some hundreds of seconds. At very earliest times the interaction lengths become very short and one might doubt the applicability of naive kinetic theory. However, as we shall see, we are mainly concerned with the epoch around t_{cmb} and we will continue to use this simplest approach.

To find the distance for the random walk, we estimate the variance *Var* in its distance from its point of origin. For a particle at light velocity, one has in a short time *dt:*

$$d(Var) = \lambda^2 dN = \lambda^2 \frac{dt}{\lambda} = \lambda\, dt, \quad (21)$$

where dN is the number of collisions in the time dt. With Equation (20), one then has for an interval up to t_{cmb}:

$$Var = \int_{t_{\mathrm{em}}}^{t_{\mathrm{cmb}}} \lambda\, dt = 4 \times 10^{11} \int_{t_{\mathrm{em}}}^{t_{\mathrm{cmb}}} (t/t_{\mathrm{rad}})^{3/2} dt\ \mathrm{s} = 8 \times 10^{30} \left(\frac{t_{\mathrm{cmb}}}{t_{\mathrm{rad}}}\right)^{5/2} \left[1 - \left(\frac{t_{\mathrm{em}}}{t_{\mathrm{cmb}}}\right)^{5/2}\right] \mathrm{s}^2. \quad (22)$$

For $t_{\mathrm{cmb}} \gg t_{\mathrm{em}}$, the last bracket may be set to one. Thus for all very early bursts the diffusion distance $\sqrt{\mathrm{Var}}$ at t_{cmb} is about the same. It has the value roughly

$$\sqrt{Var} = \sqrt{8 \times 10^{30} \left(\frac{t_{\mathrm{cmb}}}{t_{\mathrm{rad}}}\right)^{5/2}}\ \mathrm{s} \approx (4 \times 10^7)\ \mathrm{s}, \quad (23)$$

or about a light year.

Due to the short length for strong and electromagnetic interactions we arrive at a very small distance, cosmologically speaking. This justifies our view of the problem as one for a "line" in spacetime, where the gravitational field is absent, and so we can use non-general-relativistic arguments (L. D. Landau & E. M. Lifshitz 1962). If we ask over what scale the "line" picture might break down, the only dimensional scale in the cosmology is the time $a/\dot{a}$, which at t_{cmb} is about 10^{13} s. This is much more than a year, so that the system is in fact well represented by a "line." In the following we shall take the size of a "diffusive spot" at t_{cmb} to be $d \times$ lt-yr, with d a parameter of order one.

The size (Equation (23)) for the diffusive region is a constant, and does not depend on the t_{em}, while on the other hand the size for the "free flight" region (Equation (18)) does have this dependence. The qualitative reason for this difference is that the "free flight" distance results from the flight time and so involves the difference between the emission time and the absorption time. But in the random walk behavior for the diffusive spread, the rapidly increasing step size as the ambient density decreases means that the size will be determined only by the last steps. This is seen in the behavior of the integral Equation (22).

Which of the two mechanisms gives the size of a contained burst at t_{cmb} will depend on a comparison of Equation (23) (or similar calculation; T. K. Gaisser et al. 2016) with Equation (18). The results here suggest then for t_{free} being relatively early, before a time of seconds, that the "free flight" size can become less than the diffusion size.

While the exact values of the parameters can be changed in a more detailed treatment, these qualitative features may be expected to remain.

Of course, by causality neither of these distances can be larger than that for the simple noninteracting light-like flight to t_{cmb}. Comparison with Equation (17) shows this is indeed the case.

4. Some Quantities

For the different hypotheses, a few fundamental quantities are needed, which we summarize in this section. Since we will be principally concerned with effects on the CMB, we often use the scaled dimensionless time variable x:

$$x = \frac{t}{t_{\mathrm{cmb}}} = (1.1 \times 10^{-13})\, t/\ \mathrm{s}. \quad (24)$$

Since we will almost always be dealing with very early times, we will mostly have $0 < x < 1$.

4.1. Redshift to t_{cmb}

The redshift of an energy E_x given at scaled time x to the time t_{cmb} is, in view of the $a \sim t^{1/2}$ behavior of the cosmological scale factor a:

$$E_{\mathrm{cmb}} = x^{1/2} E_x. \quad (25)$$

4.2. Burst Energy

Our working assumption is that the total energy of a burst at emission is the energy within the horizon at that time (see J. Silk & L. Stodolsky 2006, Equation (29); here, the subscript "pl" refers to "Planck"), namely

$$E^{\mathrm{tot}} = M_{\mathrm{pl}} \frac{t}{t_{\mathrm{pl}}} = x\, M_{\mathrm{pl}} \frac{t_{\mathrm{cmb}}}{t_{\mathrm{pl}}} = (2 \times 10^{56})\ x\, M_{\mathrm{pl}}, \quad (26)$$

with x the scaled emission time. At t_{cmb} this energy will be, using Equation (25)

$$E_{\mathrm{cmb}}^{\mathrm{tot}} = x^{3/2}\, M_{\mathrm{pl}} \frac{t_{\mathrm{cmb}}}{t_{\mathrm{pl}}} = (2 \times 10^{56})\ x^{3/2}\, M_{\mathrm{pl}}. \quad (27)$$

The effects we shall discuss are linear in the burst energy, so if one assumes a reduced fraction of the horizon energy is more appropriate, our results can be simply multiplied by this fraction.

4.3. "Escape" Condition

The "escape condition" determines the earliest time a neutrino with a certain energy can be emitted and still propagate to late times without being absorbed. In Equation (13) there is a linear relation between the emission time and emission energy, which results in $\kappa = t_{\mathrm{free}}/t_{\mathrm{em}} = 1$.

Since there is a relatively abrupt transition around $\kappa = 1$ from "escape" to "contained" (see examples in Table 1), we take $\kappa = 1$ as defining when "escape" occurs. In terms of the scaled emission time x, the condition to "escape" is

$$x > s \times E^{\nu}_{\rm em}/{\rm GeV},\ s = 8 \times 10^{-14}. \tag{28}$$

Or, given an emission time x, the condition for a neutrino to "escape" is

$$E^{\nu}_{\rm em} < s^{-1}\, x\ {\rm GeV}. \tag{29}$$

We may also need these conditions expressed in terms of the neutrino energy at $t_{\rm cmb}$. Using $E^{\nu}_{\rm em} = x^{-1/2} E^{\nu}_{\rm cmb}$, the condition in Equation (28) becomes

$$x > (s \times E^{\nu}_{\rm cmb}/{\rm GeV})^{2/3}. \tag{30}$$

4.3.1. Very High-energy Neutrinos

Where the $x = s \times E^{\nu}_{\rm em}/{\rm GeV}$ line crosses the $x = 1$ line, (Figure 1) determines the highest-energy particles that could reach $t_{\rm cmb}$. We thus infer a maximum burst neutrino energy possible at $t_{\rm cmb}$ of

$$s^{-1}\ {\rm GeV} \sim 10^{15}\ {\rm GeV}. \tag{31}$$

This is below the Planck scale of $\sim 10^{19}$ GeV but above the highest energy observed for cosmic rays, $\sim 10^{12}$ GeV.

Neutrinos with very high energies at present are searched for by arrays like GRAND (K. Kotera 2021), AUGER (N. M. González 2023), ICECUBE (T. Gaisser & F. Halzen 2014), and KM3NeT (The KM3NeT Collaboration 2025). So far the highest neutrino energies discussed by these groups have been in the PeV (10^6 GeV) or the multi-PeV range.

Such energies at present could arise from even higher-energy bursts at early times, which are then redshifted to the present. However, because of the "escape" restriction the bursts cannot be too early. One can examine the question by using Figure 1. To use our simple formalism with $a \sim t^{1/2}$, it is best to transfer the energy to approximately $t_{\rm cmb}$, applying the suitable redshift. Thus an energy $E_{\rm now}$ observed at present could originate from an earlier (scaled) time x as given by a descending curve on the plot of $x \approx (10^3\, E_{\rm now}/E_{\rm em})^2$. When this curve enters the region below the slanted line, the neutrino cannot "escape." According to the labels on the vertical axis of the figure, the earliest time for the emission is then $x = (s\ 10^3\, E_{\rm now}/{\rm GeV})^{2/3}$. If one wishes to additionally introduce an upper limit to the possible emission energy such as the Planck scale, then this would be represented by the $E_{\rm max}$ vertical line in the figure. One then determines, for a given $E_{\rm now}$, if the descending curve encounters the $E_{\rm max}$ or "escape" restriction first.

For an example, we consider the possibility that the 10^8 GeV event of The KM3NeT Collaboration (2025) originated at even higher energy in the very early Universe. We assign it an energy of 1×10^{11} GeV at $t_{\rm cmb}$. It is possible emission energy and emission time is found on Figure 1 by following the downward curve $x = ((1 \times 10^{11})/E_{\rm em})^2$ from $x = 1$. According to the labels on the vertical axis of the figure, this curve enters the "forbidden to escape" region at $x = (s\ (1 \times 10^{11}))^{2/3} \sim (4 \times 10^{-2})$. This is then the earliest possible (scaled) emission time, where it would have had an emission energy of $\sim 10^{12}$ GeV.

That high-energy cosmic rays might originate from violent events in the very early Universe would be a new and intriguing avenue to the classic question of the origin of high-energy cosmic rays. However, due to the "escape question" it would only seem to be relevant for neutrinos, unless of course one considers "knock-on" effects from these neutrinos.

4.4. Burst Density

We will generally calculate some quantity of interest by integrating over emission energies at a given time, and then integrating over time. In doing so, the conditions for "escape" must be respected.

For the time integration we will need the density of the bursts. This density will be diluted by expansion, but since we are mainly concerned with observations of the CMB, we give it as seen at $t_{\rm cmb}$. In J. Silk & L. Stodolsky (2006) we characterized the probability of a burst per unit four-volume by the dimensionless $\mathcal{P}$, normalized (Equation 8 of J. Silk & L. Stodolsky (2006)) such that the three-density of bursts occurring at time t in an interval of cosmic time dt is $\frac{3}{64\pi t^4}\mathcal{P}(t)dt$, This normalization is such that $\mathcal{P} = 1$ would imply that the probability of a burst in the time interval $dt = t_{\rm horizon}$ and in a horizon-sized spatial volume at time t would be one. While this definition is tied to the FRW coordinate system, its normalization to the horizon size, which, as a physical quantity, gives it a certain invariant meaning. Expressed in terms of x, one has, after scaling the density as $a^3 \sim x^{3/2}$, the contribution from a time interval dx to the burst number density $\rho_{\rm bursts}$ at $t_{\rm cmb}$ is

$$d\rho_{\rm bursts} = \frac{(2 \times 10^{-41})}{{\rm s}^3} \frac{\mathcal{P}(x)}{x^{5/2}}\, dx, \tag{32}$$

where x is the scaled emission time. In assuming that $\mathcal{P}$ depends only on the time variable we make a homogeneity assumption.

The definition of $\mathcal{P}$ was motivated by the idea that the natural unit is the causal volume. The great number of casual horizon-sized regions at early times is reflected in the possibly singular behavior of Equation (32) near $x = 0$. For example, a constant $\mathcal{P}$, with a cutoff at the Planck time of 10^{-43} s would introduce a factor of 10^{84}.

Like the number of stars on a patch of the sky, the number of bursts in a region under observation does not depend on time. The question of possible time dependencies is examined in Section 9.

A symbolic representation, in only two spatial dimensions and not to scale, of the situation at $t_{\rm cmb}$ is shown in Figure 2. The large circle represents our BLC at $t_{\rm cmb}$. This indicates where features on the CMB might be observed. The large circle has a definite thickness to represent the spread in the observed region as given by $d_{\rm thom}$ the depth from which low-energy photons can escape in order to be detected (see Equation (33)). The smaller circles represent how the bursts could appear at $t_{\rm cmb}$. The larger of these represent "escape" cases where the free flight of neutrinos (or other essentially massless particles) is possible up to the time $t_{\rm cmb}$. The smallest circles represent "contained" cases where this is not possible,

that is, where the free flight distance is limited by $t_{\rm free}$. In three spatial dimensions the circles become spheres and so the intersection of the BLC and the burst regions is disk like.

4.4.1. Observational Depth

For observations via low-energy photons, as for the CMB, there will be a certain "depth" which can be observed at a given time. This is symbolized by the thickness of the big circle in Figure 2. We take this distance $d_{\rm thom}$ to be given by Thomson scattering:

$$d_{\rm thom} = \frac{1}{N_{\rm H}\,\sigma_{\rm thom}} = (6\times 10^{21})\ {\rm cm} = (2\times 10^{11})\ {\rm s}, \tag{33}$$

with $N_{\rm H}\approx (3\times 10^{2})\ {\rm cm}^{-3}$ the density of hydrogen and $\sigma_{\rm thom} = (6.6\times 10^{-25})\ {\rm cm}^2$ the Thomson cross section.

4.4.2. Number of Bursts in an Observation

Equation (32) refers to the number of bursts per unit three-volume. For a given observational arrangement, the observed three-volume will be determined by the angular acceptance of the observations, which lead to a linear dimension on the CMB, $l_{\rm acc}$, and the depth $d_{\rm thom}$ from which photons can escape, as conditioned by Thomson scattering. Thus the volume observed (by means of low-energy photons) is

$$V_{\rm obs} = l_{\rm acc}^2 d_{\rm thom}. \tag{34}$$

Hence the number of bursts originating from a scaled time interval dx is

$$dn = V_{\rm obs}\times \frac{(2\times 10^{-41})}{{\rm s}^3}\frac{\mathcal{P}(x)}{x^{5/2}}dx. \tag{35}$$

For, say milli-radian angular acceptance, one has $l_{\rm acc} = (9\times 10^{11})$ s and with $d_{\rm thom} = (2\times 10^{11})$ s one has $V_{\rm obs} = (2\times 10^{35})\ {\rm s}^3$.

4.5. Burst Energy Production

We can use Equation (32) to express the total energy produced by the bursts. Each burst has an energy, according to Equation (26), $E^{\rm tot} = (2\times 10^{56})xM_{\rm pl}$, where x is the scaled emission time. Since the energy undergoes a redshift, it must be referred to some time or frame. We chose to express it in terms of the value it would have at $t_{\rm cmb}$. According to Equation (25) the redshift introduces a factor of $x^{1/2}$, thus giving an $x^{3/2}$ behavior. Then combining with Equation (32) one has at $t_{\rm cmb}$ the contribution to the energy density $\epsilon_{\rm bursts}$ coming from the bursts:

$$\begin{aligned} d\epsilon_{\rm bursts} &= (2\times 10^{56})\,x^{3/2}\frac{M_{\rm pl}}{{\rm s}^3} \\ &\quad\times (2\times 10^{-41})\,\frac{\mathcal{P}(x)}{x^{5/2}}dx \\ &= (3\times 10^{15})\,\frac{M_{\rm pl}}{{\rm s}^3}\frac{\mathcal{P}(x)}{x}dx. \end{aligned} \tag{36}$$

Integrating this will give the energy density from the bursts, expressed at $t_{\rm cmb}$. It is noteworthy that the potentially strong singularity at $x=0$ has becomes only logarithmic when considering the energy density. This conclusion was anticipated in J. Silk & L. Stodolsky (2006, see Section 3, "Olber's Paradox").

5. "Escape," Illustrative Models

As one sees from Table 1 or Figure 1, if neutrinos which are produced very early or with high energy will generally interact before $t_{\rm cmb}$, they will not "escape." However, in this section we discuss how bursts, or parts of bursts, may indeed propagate freely to $x=1$ or $t_{\rm cmb}$.

The parameters involved, especially $t_{\rm free}$, depend on the particle emission energy. To examine the effects of this spectrum, we consider two simple models, one with a well-defined energy for the burst particles and one with a spread-out spectrum. We carry out the analysis using neutrino parameters, and estimate two quantities: the total energy delivered to $t_{\rm cmb}$ and the energy spectrum at that time. To obtain these quantities at other times one may rescale the densities or energies. For the present time instead of at $t_{\rm cmb}$, one would use $a(t_{\rm cmb})^3 = (1\times 10^{-9})$ for density and rescale energies by $a(t_{\rm cmb}) = (1\times 10^{-3})$.

5.1. General Formulas

Before turning to the models, we note it is possible to give general formulas in terms of the spectral energy density at emission. That is, since a burst can contain a range of energies, we introduce the quantity $\mathcal{E}$ for the spectrum of the energy. That is, the part of the energy in a single burst, contained in an interval of particle energy at emission $dE^{\nu}_{\rm em}$ is

$$\mathcal{E}(E^{\nu}_{\rm em})dE^{\nu}_{\rm em}. \tag{37}$$

With this definition, one has

$$\int_0^{\infty}\mathcal{E}\,dE_{\rm em} = E^{\rm tot}, \tag{38}$$

which is given by Equation (26). $\mathcal{E}$ can also depend on the time variable, in general. $\mathcal{E}$ is dimensionless, being the ratio of two energies. If we prefer to think in terms of particle number N instead of spectral energy density, one can write the pulse energy as the product of the number of particles times their individual energy $dE^{\nu}_{\rm em}\mathcal{E} = E^{\nu}_{\rm em}dN$, so that

$$\frac{dN}{dE^{\nu}_{\rm em}} = \frac{1}{E^{\nu}_{\rm em}}\mathcal{E}. \tag{39}$$

5.1.1. Energy Density

The energy reaching $t_{\rm cmb}$ from one pulse at emission time x, taking those energies that escape from Equation (29), and applying the redshift, is

$$x^{1/2}\int_0^{ul}\mathcal{E}\,dE_{\rm em} = x^{1/2}\mathcal{I}(x), \tag{40}$$

calling the integral $\mathcal{I}$, which is an energy

$$\mathcal{I} = \int_0^{ul}\mathcal{E}\,dE_{\rm em}. \tag{41}$$

The upper limit ("ul") can be the "escape" limit for that x, namely x/s GeV, or some limit on the emission energy $E_{\rm max}$. $\mathcal{I}$ can depend on the time variable x both through the limit of integration and through $\mathcal{E}$. Now using Equation (32), we have

finally for the escaping burst energy density $\epsilon^{\rm esc}_{\rm bursts}$ at $t_{\rm cmb}$:

$$\epsilon^{\rm esc}_{\rm bursts} = \frac{(2\times 10^{-41})}{\rm s^3}\int_0^1 dx\ \mathcal{I}(x)\frac{\mathcal{P}(x)}{x^2}dx. \tag{42}$$

5.1.2. Spectrum

In addition to the total "escape" energy density, another quantity of interest is the spectrum of the neutrinos, i.e., how they are distributed with respect to energy. This information is contained in $\mathcal{E}$, which must be redshifted to $t_{\rm cmb}$. We note that both the numerator and the denominator in Equation (37) redshift the same way, so the ratio is unchanged by the redshift. We thus have, at $t_{\rm cmb}$, for a single pulse, expressed in terms of $E^{\nu}_{\rm cmb}$ the burst energy contained in the interval $dE^{\nu}_{\rm cmb}$:

$$\mathcal{E}(E^{\nu}_{\rm em})\,dE^{\nu}_{\rm cmb} = \mathcal{E}(x^{-1/2}E^{\nu}_{\rm cmb})\,dE^{\nu}_{\rm cmb}, \tag{43}$$

where $\mathcal{E}$ is still the spectrum at emission. Summing over all times x by means of Equation (32), the integral is from the earliest time possible for the energy in question to $x = 1$.

Then the energy density per unit particle energy $dE^{\nu}_{\rm cmb}$ at $t_{\rm cmb}$, as a function of particle or neutrino energy $E^{\nu}_{\rm cmb}$, is

$$\frac{d\epsilon^{\rm esc}_{\rm bursts}}{dE^{\nu}_{\rm cmb}} = \frac{(2\times 10^{-41})}{\rm s^3}\int_{x_{\rm min}}^1 \mathcal{E}(x^{-1/2}E^{\nu}_{\rm cmb})\frac{\mathcal{P}(x)}{x^{5/2}}dx, \tag{44}$$

where $x_{\rm min}$ is the earliest time from which the $E^{\nu}_{\rm cmb}$ under consideration can originate. When this is given by the "escape" condition then $x_{\rm min} = (s\times E_{\rm cmb})^{2/3}$. Or if it is given by the $E_{\rm max}$ limitation, $x_{\rm min} = (E_{\rm cmb}/E_{\rm max})^2$. Which limit applies depends on the $E^{\nu}_{\rm cmb}$ under consideration (see Figure 1).

5.2. Models

From the above general formulas, the total energy density or the energy spectrum can be evaluated from models or information on $\mathcal{P}$, I. The deduction of the neutrino spectrum associated with a burst is undoubtedly a complicated matter, involving both the primary process and the characteristics of the ambient medium. However, to exemplify the role of the various factors involved, we will consider some very simple—probably oversimplified—models. In the first model we assume that the neutrino emission is concentrated around a well-defined emission energy $\bar{E}^{\nu}$. In the second model, we take the opposite case, where the neutrino energy at emission is uniformly spread out, up to some $E_{\rm max}$. Finally, we mention a third case where the emission all takes place at essentially a given cosmic time.

5.2.1. Well-defined Emission Energy

A situation which can be examined in a straightforward manner is that in which the neutrino energy at emission has a relatively well-defined value, which we call $\bar{E}^{\nu}$. While the neutrino pulse will of course have a spread of energies at emission, we assume in this model that this spread is not large, compared to the average particle energy in the pulse $\bar{E}^{\nu}$. We will then approximate the situation with a unique energy for the neutrinos at emission, with value $\bar{E}^{\nu}$.

In this approximation the integral over $E^{\nu}_{\rm em}$ may simply be replaced by $E^{\rm tot}$, Equation (38). However, in Figure 1, below where the exclusion line $x = sE^{\nu}_{\rm em}/{\rm GeV}$ would cross an $\bar{E}^{\nu}$ vertical band, the neutrinos cannot escape. Thus for $\mathcal{I}$ we simply have

$$\begin{aligned}\mathcal{I} &= E^{\rm tot}_{\rm em} \qquad x > s\times \bar{E}^{\nu}/{\rm GeV},\\ \mathcal{I} &= 0 \qquad\quad x < s\times \bar{E}^{\nu}/{\rm GeV}.\end{aligned} \tag{45}$$

Energy density. With $E^{\rm tot}$ given by Equation (26), the integral for the total energy density to $t_{\rm cmb}$ is given by Equation (42) and one has for the burst energy density escaping to $t_{\rm cmb}$:

$$\begin{aligned}&\frac{(2\times 10^{-41})}{\rm s^3}\int_{s\times\bar{E}^{\nu}/{\rm GeV}}^1 dx\ E^{\rm tot}_{\rm em}\frac{\mathcal{P}(x)}{x^2}\\ &= \frac{(3\times 10^{15})}{\rm s^3}M_{\rm pl}\int_{s\times\bar{E}^{\nu}/{\rm GeV}}^1 dx\ \frac{\mathcal{P}(x)}{x}\\ &= \frac{(4\times 10^{34})}{\rm s^3}\,{\rm GeV}\times\int_{s\times\bar{E}^{\nu}/{\rm GeV}}^1 dx\ \frac{\mathcal{P}(x)}{x}.\end{aligned} \tag{46}$$

$\mathcal{P}$ and $\bar{E}^{\nu}$ *constant*. If one were to make the further drastic simplification that $\mathcal{P}$ and $\bar{E}^{\nu}$ are constant in time, one would get for the burst energy density at $t_{\rm cmb}$:

$$\epsilon^{\rm esc}_{\rm bursts} = \frac{(4\times 10^{34})}{\rm s^3}\,{\rm GeV}\,\mathcal{P}(\ln(1/{\rm s}) - \ln(\bar{E}^{\nu}/{\rm GeV}). \tag{47}$$

This can be compared with the standard $(\pi^2/15)T^4 = (8\times 10^{33})$ GeV s^{-3} for the radiant energy density at $t_{\rm cmb}$. Thus if $\mathcal{P}$ is relatively large, this energy could be significant. However we stress that a basic assumption of our calculations is that $\mathcal{P}$ is sufficiently small that the standard cosmology is essentially unaffected. For some discussion of this see the beginning of Section 10.

Neutrino spectrum. With the simplification in this model of a definite energy $\bar{E}^{\nu}$, we can also evaluate the form of the neutrino energy spectrum at $t_{\rm cmb}$ from Equation (44). Approximating the energy spectrum density by a δ function at $\bar{E}^{\nu}$, one has $\mathcal{E} = E^{\rm tot}\delta(\bar{E}^{\nu} - E_{\rm em})$ so that Equation (44) for the total energy density per interval of $dE^{\nu}_{\rm cmb}$ becomes

$$\begin{aligned}\frac{d\epsilon^{\rm esc}_{\rm bursts}}{dE^{\nu}_{\rm cmb}} &= \frac{(3\times 10^{15})}{\rm s^3}M_{\rm pl}\int_{x_{\rm min}}^1 \delta(\bar{E}^{\nu}\\ &\quad - x^{-1/2}E^{\nu}_{\rm cmb})\frac{\mathcal{P}(x)}{x^{3/2}}dx.\end{aligned} \tag{48}$$

Taking into account the Jacobian for $x^{-1/2}E^{\nu}_{\rm cmb}$ in the δ function, which is $2x^{3/2}/E^{\nu}_{\rm cmb}$, one obtains

$$\frac{d\epsilon^{\rm esc}_{\rm bursts}}{dE^{\nu}_{\rm cmb}} = \frac{(6\times 10^{15})}{\rm s^3}\frac{M_{\rm pl}}{E^{\nu}_{\rm cmb}}\mathcal{P}(1 - x_{\rm min}), \tag{49}$$

with $x_{\rm min} = (s\times\bar{E}^{\nu}/{\rm GeV})^{2/3}$ as given by Equation (30). For $x_{\rm min} > 1$ the expression is to be taken as zero. $\mathcal{P}$ is to be evaluated at the scaled time $x = (E^{\nu}_{\rm cmb}/\bar{E}^{\nu})^2$. Using Equation (39), this may be also converted to a particle number spectrum:

$$\frac{dN^{\rm esc}}{dE^{\nu}_{\rm cmb}} = \frac{(6\times 10^{15})}{\rm s^3}\frac{M_{\rm pl}}{(E^{\nu}_{\rm cmb})^2}(1 - x_{\rm min})\mathcal{P}, \tag{50}$$

where $N^{\rm esc}$ is the number density of "escaped" particles. For a not too rapidly varying $\mathcal{P}$, an E^{-2} behavior is expected. We note this is quite different from a thermal distribution, where there is an exponential cutoff with temperature.

There is of course a high-energy cutoff in this model, for $E^{\nu}_{\rm cmb} > \bar{E}^{\nu}$, since the redshift of $\bar{E}^{\nu}$ can only lead to lower

energies. However there is also a low-energy cutoff since there is a smallest x that can contribute, namely $x_{\rm min}$. From the redshift this lowest $E^{\nu}_{\rm cmb}$ is $x^{1/2}_{\rm min}\bar{E}^{\nu} = \bar{E}^{\nu}\,(s\bar{E}^{\nu}\,/{\rm GeV})^{1/2}$. In Figure 1 this corresponds to a situation where a vertical $\bar{E}^{\nu}$ band would cross a curve at a point below the $x = sE_{\rm em}$ line. One thus finds, in this model, that the narrow energy band around $\bar{E}^{\nu}$ at emission becomes, through the spread in emission times, the band

$$\bar{E}^{\nu}\,(s\bar{E}^{\nu}\,/{\rm GeV})^{1/2} < E^{\nu}_{\rm cmb} < \bar{E}^{\nu}, \tag{51}$$

at $t_{\rm cmb}$. When we have $(s\bar{E}^{\nu}\,/{\rm GeV}) > 1$, then all emission possibilities are "under water," i.e., below the suppression line $x = sE_{\rm em}/{\rm GeV}$ on Figure 1. Since s is a small number, (Equation (28)), it seems that a wide range of $\bar{E}^{\nu}$ is possible within this model. When the emission spectrum contains neutrinos down to arbitrarily low energy, as discussed for the "spread-out" model below, a lower limit as in Equation (51), does not occur.

5.2.2. Large Energy Spread Model

In the previous Section 5.2.1, we made the simplifying assumption that that there was a well-defined common energy for the neutrinos in a burst. Here we examine the opposite case, with a very spread-out neutrino distribution, reaching down to zero energy. In this model, unlike in the first model, there is no earliest escape time since the bursts contain arbitrarily low-energy neutrinos. Also lower-energy and thus "escaping" particles need not come from higher redshift, as was the case before.

As an example, we assume that at emission the total energy in each interval of particle energy is constant, up to some $E_{\rm max}$:

$$\begin{aligned}&\mathcal{E} = {\rm constant}{=}\frac{E^{\rm tot}}{E_{\rm max}} {\rm for}\ E^{\nu}_{\rm em} < E_{\rm max},\\ &\mathcal{E} = 0\ {\rm for}\ E^{\nu}_{\rm em} > E_{\rm max}.\end{aligned} \tag{52}$$

This is like the spectrum for bremsstrahlung photons, perhaps the "most spread out" of familiar particle spectra. The value of the constant follows from the fact that the integral over $\mathcal{E}$ should be $E^{\rm tot} = xM_{\rm pl}(2\times 10^{56})$.

To find the total burst energy to $t_{\rm cmb}$ we note that in this model all the neutrinos in a burst will "escape" if $x > sE_{\rm max}/{\rm GeV}$ (see Figure 1):

$$\mathcal{I} = E^{\rm tot}\ x > sE_{\rm max}/{\rm GeV}, \tag{53}$$

and otherwise only the part up to the escape energy enters

$$\mathcal{I} = E^{\rm tot}\frac{(x/s)\,{\rm GeV}}{E_{\rm max}}\ x < sE_{\rm max}/{\rm GeV}. \tag{54}$$

Inserting in Equation (42) gives the total escaped burst energy density at $t_{\rm cmb}$:

$$\begin{aligned}&\frac{(2\times 10^{-41})}{{\rm s}^3}\int_0^1 dx\ \ \mathcal{I}(x)\frac{\mathcal{P}(x)}{x^2}dx = \frac{(3\times 10^{15})}{{\rm s}^3}M_{\rm pl}\\ &\times\left(\int_{s\,E_{\rm max}/{\rm GeV}}^1\frac{\mathcal{P}(x)}{x}dx\right.\\ &\left.+\frac{1}{sE_{\rm max}/{\rm GeV}}\int_o^{s\,E_{\rm max}/{\rm GeV}}\mathcal{P}(x)dx\right).\end{aligned} \tag{55}$$

This formula applies for $sE_{\rm max}/{\rm GeV} < 1$, meaning there is some time before $x = 1$ when the $E_{\rm max}$ neutrinos escape, when the full neutrino burst escapes. When this is not true, when for all times $x < 1$, only a part of the burst escapes, then the first term is absent and we simply have the total escaped burst energy density at $t_{\rm cmb}$:

$$\epsilon^{\rm esc}_{\rm bursts} = \frac{(3\times 10^{15})}{{\rm s}^3}M_{\rm pl}\frac{1}{sE_{\rm max}/{\rm GeV}}\int_o^1\mathcal{P}(x)dx. \tag{56}$$

Since s is small, which condition would apply depends essentially on $E_{\rm max}$.

Energy with constant $\mathcal{P}$. Assuming constant $\mathcal{P}$ for illustration, one can evaluate Equation (55) explicitly to get for the burst energy density at $t_{\rm cmb}$:

$$\epsilon^{\rm esc}_{\rm bursts} = \frac{(3\times 10^{15})}{{\rm s}^3}M_{\rm pl}\mathcal{P}(\ln(1/(sE_{\rm max}/{\rm GeV})) + 1), \tag{57}$$

where again with $sE_{\rm max}/{\rm GeV} > 1$ the log term is absent and one has for the escaped burst energy density at $t_{\rm cmb}$:

$$\epsilon^{\rm esc}_{\rm bursts} = \frac{(3\times 10^{15})}{{\rm s}^3}M_{\rm pl}\mathcal{P}\frac{1}{sE_{\rm max}/{\rm GeV}}, \tag{58}$$

showing how a large $E_{\rm max}$ or spread reduces the "escape."

In this model we can give the energy spectrum using Equation (44), so the energy density per unit $dE^{\nu}_{\rm cmb}$ is

$$\frac{d\epsilon^{\rm esc}_{\rm bursts}}{dE^{\nu}_{\rm cmb}} = \frac{(2\times 10^{-41})}{{\rm s}^3}\int_{x_{\rm min}}^1\mathcal{E}(x^{-1/2}E^{\nu}_{\rm cmb})\frac{\mathcal{P}(x)}{x^{5/2}}dx, \tag{59}$$

where $x_{\rm min}$ is the earliest time $E^{\nu}_{\rm cmb}$, in view of the escape condition, can come from, namely $x_{\rm min} = (sE^{\nu}_{\rm cmb}/{\rm GeV})^{2/3}$. In the present model we have for $\mathcal{E}$ for a given $E^{\nu}_{\rm cmb}$ as a function of x:

$$\begin{aligned}&\mathcal{E} = \frac{E^{\rm tot}}{E_{\rm max}} \qquad {\rm for}\ x^{1/2} > \frac{E^{\rm cmb}}{E_{\rm max}},\\ &\mathcal{E} = 0 \qquad\quad {\rm for}\ x^{1/2} < \frac{E^{\rm cmb}}{E_{\rm max}}.\end{aligned} \tag{60}$$

There are then two possible lower limits ("*ll*"), on the x integration; either $x_{\rm min}$ or the second of Equation (60), according to which is larger. Then inserting $\mathcal{E}$ gives

$$\frac{d\epsilon^{\rm esc}_{\rm bursts}}{dE^{\nu}_{\rm cmb}} = \frac{(3\times 10^{15})}{{\rm s}^3}\frac{M_{\rm pl}}{E_{\rm max}}\int_{ll}^1\frac{\mathcal{P}(x)}{x^{3/2}}dx, \tag{61}$$

where "*ll*" is the larger of $(x\ E^{\nu}_{\rm cmb}/{\rm GeV})^{2/3}$ or $(E^{\nu}_{\rm cmb}/E_{\rm max})^2$. It can be seen that the two become equal where the escape line crosses the $E_{\rm max}$ line, that is for $x = sE_{\rm max}/{\rm GeV}$, or in terms of $E^{\nu}_{\rm cmb}$, for $E^{\nu}_{\rm cmb} = E_{\rm max}(sE_{\rm max}/{\rm GeV})^{1/2}$. The situation is sketched in Figure 1.

Constant $\mathcal{P}$. Making the assumption of constant $\mathcal{P}$ for illustration, one then has for the total energy density in $dE^{\nu}_{\rm cmb}$:

$$\begin{aligned}&\frac{d\epsilon^{\rm esc}_{\rm bursts}}{dE^{\nu}_{\rm cmb}} = \frac{(6\times 10^{15})}{{\rm s}^3}\frac{M_{\rm pl}}{E_{\rm max}}\mathcal{P}\\ &\times\left(\frac{E_{\rm max}}{E^{\nu}_{\rm cmb}} - 1\right) \qquad E^{\nu}_{\rm cmb} > E_{\rm max}\times(sE_{\rm max}/{\rm GeV})^{1/2}\\ &\times((sE^{\nu}_{\rm cmb}/{\rm GeV})^{-1/3} - 1) \quad E^{\nu}_{\rm cmb} < E_{\rm max}\times(sE_{\rm max}/{\rm GeV})^{1/2}.\end{aligned} \tag{62}$$

With the value $\sim 10^{-15}$ for s, the first option falls away for $E_{\rm max} > 10^{15}$ GeV and the second variant must be used for all

energies $E^{\nu}_{\rm cmb}$. For very large $E_{\rm max}/E^{\nu}_{\rm cmb}$, which seems plausible for this model and for cases where the first option still applies, we can further simplify to obtain

$$\frac{d\epsilon^{\rm esc}_{\rm bursts}}{dE^{\nu}_{\rm cmb}} = \frac{(6\times 10^{15})}{\rm s^3}\mathcal{P}\frac{M_{\rm pl}}{E^{\nu}_{\rm cmb}},$$
$$E^{\nu}_{\rm cmb} > E_{\rm max}\times (sE_{\rm max}/{\rm GeV}). \quad (63)$$

All these formulas may be expressed in terms of a particle number density by $E^{\nu}_{\rm cmb}\rightarrow (E^{\nu}_{\rm cmb})^2$ as in Equation (39).

5.3. Low-energy Early Burst Neutrinos at Present

While many assumptions and approximations were made, a few conclusions are suggested from the models. One is that, in general, a low-energy peak in the burst neutrino spectrum is to be anticipated. This reflects the higher probability for a low-energy neutrino to "escape," combined with the growing number of potential emission regions at early times, Equation (32), where the neutrinos undergo a very large redshift.

Such neutrinos from very early times will become very low-energy particles at present. With some neutrino mass, some or all of them will likely be nonrelativistic. As one sees from the third column of Table 1, it is quite possible that the very early burst neutrinos become nonrelativistic, even if they have only millivolt masses. It therefore appears that a prediction of the burst model with neutrinos, as we have discussed in this section, is that there is at present a nonthermal population of low-energy neutrinos, with some or all of them nonrelativistic. These would be in addition to the thermal $\sim$2 K neutrinos expected (S. Weinberg 1972) in any case from the standard cosmology.

In addition, in some of our estimates, as in Equation (50), there is a power-law $\sim 1/E^2$ behavior of the neutrino spectrum. This is quite different from the exponential cutoff in a thermal spectrum. The difficult question of the detection of relic neutrinos has a long and interesting history (S. Weinberg 1962; L. Stodolsky 1975;[5] E. Vitagliano et al. 2020).

5.4. Definite Emission Time Model

A different type of simple model that might be used to illustrate some features of the question is one where the bursts essentially all originate around the same cosmic time. That is, we can approximate $\mathcal{P}(t)\sim\delta(t-t_{\rm em})$.

The most important aspect of such a situation would be the value of the emission time $t_{\rm em}$. This time will determine the redshift to $t_{\rm cmb}$ so that the energies will be shifted according to Equation (25). If $t_{\rm em}$ is very early, x is very small and the particle energies at $t_{\rm cmb}$ are very small. For example in the model with the given emission energy $\bar{E}^{\nu}$, one will have

$$E_{\rm cmb} = x^{1/2}\bar{E}^{\nu}, \quad (64)$$

where x is $t_{\rm em}/t_{\rm cmb}$ (Equation (24)). If this downshift is large enough, say to less than 1 MeV, the neutrinos will not be able to interact inelastically and we would arrive to the situation mentioned in Section 5.3 where they escape to the present, forming a nonthermal relic neutrino background. This would also mean that the positron mechanism, to be discussed in Section 6, is not possible. With a spread spectrum this reasoning will apply to that part of the spectrum, which is downshifted below the inelastic threshold.

An important change vis a vis the previous discussions would concern $t_{\rm free}$. With $t_{\rm em}$ fixed, the only variability in Equation (11) is in the energy factor. Thus if all the bursts are essentially similar, $t_{\rm free}$ would be the same for all bursts. Thus the smallest circles in Figure 2 would all be of about the same size, and not variable as in situations with a distribution of emission times. By the same token, approximately fixed values for $t_{\rm free}$ and $t_{\rm em}$ for all bursts would mean that κ, governing "escape" or "confinement," is the same for all of them.

These considerations may be visualized on Figure 1. Draw a horizontal line at the scaled time for $t_{\rm em}$. Along this line denotes the emission energy (energies). If the resulting point(s) are below the slanted line the particles do not "escape." If they are above the slanted line, construct curves like I or II starting from the points. Where the curves cross the $x=1$ ordinate gives their energy at $t_{\rm cmb}$.

Concerning intensities in this model, let us express the δ function hypothesis in terms of the scaled emission time $x_{\rm em}$, so that $\mathcal{P}\approx\mathcal{P}_o\,\delta(x-x_{\rm em})$, where $\mathcal{P}_o$ is a dimensionless magnitude factor. Then according to Equation (32) we have a number density of bursts at $t_{\rm cmb}$:

$$\rho_{\rm bursts} = \frac{(2\times 10^{-41})}{\rm s^3}\frac{\mathcal{P}_o}{x_{\rm em}^{5/2}}. \quad (65)$$

As an example, we could apply this to the situation just mentioned, where the neutrinos are below the inelastic threshold and escape to the present to form part of the relic neutrino background. In the situation with a more or less definite energy at emission $\bar{E}^{\nu}$, one has for the number of neutrinos in a burst according to Equation (26):

$$(2\times 10^{56})\,x_{\rm em}\frac{M_{\rm pl}}{\bar{E}^{\nu}}. \quad (66)$$

Multiplying by Equation (65) and a factor of 10^{-9} for the redshift of the density to the present, one has finally

$$N^{\rm now} = \frac{(4\times 10^{6})}{\rm s^3}\frac{M_{\rm pl}}{\bar{E}^{\nu}}\cdot\frac{\mathcal{P}_o}{x_{\rm em}^{3/2}} \quad (67)$$

for the present density of relic burst neutrinos, in this model.

6. Positrons

If neutrinos in the MeV range or above arrive at relatively late times like $t_{\rm cmb}$ or afterwards, the production of positrons, whose annihilation could give an observable signal, is possible.

The detection of such a signal would be very characteristic of the bursts, since with only $\sim$1 eV or less, for the thermal energies present in the purely equilibrium picture, positrons should be absent. That is we consider

$$\bar{\nu}+p\rightarrow e^{+}+n \qquad e^{+}+e^{-}\rightarrow\gamma+\gamma, \quad (68)$$

giving 511 keV photons. Redshifted to the present time, these should give soft X-rays. Below we attempt a more detailed estimate of the redshift of the annihilation photons.

Other reactions which lead to positrons via decay chains, such as $\overline{\nu_{\mu}}\rightarrow\mu^{+}$, or the production of π^{+} mesons could also contribute, but Equation (68) has the lowest threshold and should be the most significant. In principle there is also a 2.2 MeV γ-ray signal from capture of a neutron on hydrogen,

[5] Adjustments of some factors according to the parameters of the modern Electro-Weak Standard Model are given in G. Duda et al. 2001.

but due to the low matter density at $t_{\rm cmb}$ or later the 14 minute decay of the neutron is much faster.

6.1. Conversion Probability

While of course positrons will be produced all along the path of a neutrino pulse, only those conversions which are close enough so that that the annihilation photon can "escape" to the present time are potentially observable.

It is possible to give an estimate for the probability of such a conversion without entering into details of the intervening matter distribution. This is because the same atoms or matter density responsible for stopping the outgoing annihilation photons are also the relevant targets for the production reaction (Equation (68)). Only when Equation (68) takes place within the last mean free path for the photon will the photons "escape." If τ is the column density for this last mean free path, it is given by the condition $\tau\sigma_\gamma(500\,\mathrm{keV}) \approx 1$, or $\tau \approx 1/\sigma_\gamma(500\ \mathrm{keV})$. On the other hand the probability for a positron to be produced in this region is $\tau\sigma_{\nu\to e^+}$. Thus τ cancels and one is simply left with the ratio of the cross sections.

Thus the conversion probability C for a neutrino to lead to an observable photon is expected to be

$$C = \frac{\sigma_{\nu\to e^+}}{\sigma_\gamma(500\,\mathrm{keV})} = \frac{(1\times 10^{-38})\,(E^\nu/\mathrm{GeV})\mathrm{cm}^2}{(2.8\times 10^{-25})\ \mathrm{cm}^2} \approx (3\times 10^{-14})\,(E^\nu/\mathrm{GeV}), \tag{69}$$

where we used $\sigma_{\nu\to e} = (1.0\times 10^{-38})\,(E^\nu/\mathrm{GeV})\,\mathrm{cm}^2$, with E^ν the energy of the neutrinos at the conversion time. For $\sigma_\gamma(500\ \mathrm{keV})$ see Equation (73).

6.2. Redshift of the Photon

While the above argument shows that for an estimate of the conversion probability it is not necessary to know the exact locus where Equation (68) takes place, we would also like to know the energy of the annihilation photon at present. For this it is necessary to determine the epoch where the positrons are produced to find the redshift of the 511 keV photons.

The quantity of interest is $N_\gamma(t_{\rm now})$, the present density of annihilation photons, which gives our detection rate. In particular we are interested in its energy spectrum $\frac{dN_\gamma(t_{\rm now})}{d\omega}$, where ω is the present energy of an annihilation photon.

Although the annihilation of a positron on a stationary electron leads to a "line" at 511 keV, various effects lead to a spread of the photon spectrum. There is the thermal motion of the atoms and the motion of the bound electron in the atom. However, the most important effect in our present problem will be due to the spread of the redshifts in the origin of the γ ray. There is an essentially one-to-one relation between the redshift of the origin z and ω:

$$\omega = (1/z)\ 511\ \mathrm{keV}\ d\omega = (2/3) z^{1/2}\frac{dt}{t_{\rm now}}\ 511\ \mathrm{keV}. \tag{70}$$

Since we will find that the relevant times are well into the matter-dominated epoch, for z we use $z = (t_{\rm now}/t)^{2/3}$, with $t_{\rm now} = (2.8\times 10^{17})$ s (J. Silk & L. Stodolsky 2006). The second relation shows how a spread in production times dt gives a band of present energies $d\omega$.

A time interval dt at redshift z thus gives a contribution to the present density of the annihilation photons with energy $\omega = (1/z)\ 511$ keV:

$$dN_\gamma(t_{\rm now}) = K(z)dt = K(z)\frac{1}{z^{1/2}}\,(3/2)\frac{t_{\rm now}}{511}\,d\omega, \tag{71}$$

where K is a factor for the conversion of neutrinos into photons, involving the local fluxes, cross sections, and propagation to the present.

6.2.1. Absorption Factor

The most important element in K is the attenuation factor for the initially 511 keV photon. That is, the probability of an emitted photon to reach us is governed by a factor $\mathcal{A}$:

$$\mathcal{A} = \exp(-\tau/\tau_o), \tag{72}$$

where τ is the column density or "thickness" of the matter traversed, and τ_o is a parameter characterizing the matter. This parameter is usually given in g cm^{-2} and for 500 eV photons in hydrogen one has[6]

$$\tau_o \approx 6\ \mathrm{g\ cm}^{-2}. \tag{73}$$

By referring to the mass of the hydrogen atom or proton instead of grams, Equation (73) may also be expressed as an effective cross section namely $\sigma_\gamma(500\,\mathrm{keV}) = (2.8\times 10^{-25})\ \mathrm{cm}^2$, which we used in Equation (69). The mass absorption parameter or cross section is energy dependent and so will vary somewhat during the flight of the photon as its energy is redshifted. However, most of the absorption will take place close to the emission time and we simply use the values for absorption at 500 keV.

To evaluate Equation (72) in the cosmological situation, we take the intervening matter to be essentially hydrogen and estimate the column density from the present back to a time t or equivalently to an $a(t)$ or $z = 1/a$. One first needs the density, which we take to be

$$\rho(t) = \rho_o\left(\frac{t_{\rm now}}{t}\right)^2, \tag{74}$$

where ρ_o is the present density of hydrogen and the density scales as $1/a^3$, using $a = (t/t_{\rm now})^{2/3}$.

One thus has for the column density

$$\tau = \int_{t_{\rm now}}^{t}\rho(t)dt = \rho_o t_{\rm now}\left(\frac{t_{\rm now}}{t}\right) = \rho_o t_{\rm now}\times a^{-3/2} = \rho_o\, t_{\rm now}\times z^{3/2}, \tag{75}$$

and for the absorption factor expressed in terms of z:

$$\mathcal{A} = \exp\left(-\frac{\rho_o\, t_{\rm now}}{6\ \mathrm{g\ cm}^{-2}}\, z^{3/2}\right) = \exp(-(7\times 10^{-4})\ z^{3/2}) = \exp(-(z/z_o)^{3/2}), \tag{76}$$

where we introduce the quantity $z_o = \left(\frac{\rho_o\, t_{\rm now}}{6\ \mathrm{g\ cm}^{-2}}\right)^{-2/3} \approx 130$, which characterizes the absorption distance in terms of z. We have taken ρ_o at 5% of the critical density, namely $\rho_o = (5\times 10^{-31})\ \mathrm{g\ cm}^{-3}$.

[6] See the "X-ray mass attenuation tables" of NIST, available at physics.nist.gov/PhysRefData/XrayMassCoef/ElemTab/z01.html. We consider only hydrogen; the contribution from helium may be seen to be small.

6.2.2. Spectrum

In addition to $\mathcal{A}$, which favors nearby reactions, there are countervailing factors favoring higher redshift for Equation (68). These include the higher densities and the smaller downshift of the neutrino energy.

We anticipate that these various effects will lead to a cumulative power $\sim z^p$, so that the distribution of origin z values for a presently observable annihilation photon is proportional to

$$z^p\mathcal{A} = z^p \times \exp(-(z/z_o)^{3/2}). \tag{77}$$

This product of increasing and decreasing functions leads to a peak at some z, namely at $z = \left(\frac{2}{3}p\right)^{2/3} \times z_o$.

As for the value of p, the increasing density of target protons gives a factor of z^3. The incoming neutrino flux will also increase by $\sim z^3$ but this is canceled by a factor of $1/z^3$ for the produced photon density, by the redshift to the present. This cancellation reflects the fact that photon and neutrino densities redshift in the same way.

As for the neutrino energy factor, this will depend on whether we are in the fully relativistic regime $E > 1\,\mathrm{GeV}$ where the cross section is linear with energy, or at lower energy, where the behavior is closer to quadratic (J. A. Formaggio & G. P. Zeller 2012). With the $1/z^{1/2}$ factor from Equation (71), this leads to $p \approx 3.5$–4.5 and so

$$z_{\mathrm{peak}} \approx (1.8-2.1)z_o \approx (230-280), \tag{78}$$

implying that the original 511 keV photon appears around $511\,\mathrm{keV}/z_{\mathrm{peak}}$ that is as a soft, $\sim$2 or 3 keV range X-ray.

An important question is the width to be expected in the observed photon spectrum, since this can be significant in separating the signal from the backgrounds. Substituting $z = 511\,\mathrm{keV}/\omega$ for z in Equation (77), one finds a rather broad distribution in ω:

$$\frac{dN_\gamma(t_{\mathrm{now}})}{d\omega} \sim (1/\omega)^p \exp(-(3.9/\omega)^{3/2}). \tag{79}$$

Due to the spread in the redshift of origin the "line" has become a broad and somewhat asymmetric "bump."

6.3. Intensity

Finally, one would like to have an estimate of the intensity of the signal, which is the expected number density of the annihilation photons at present, $N_\gamma(t_{\mathrm{now}})$. This will of course depend crucially on the nature and frequency of the bursts, but to see the interplay of the various elements, we can examine some of our simple schematic models.

A simple estimate follows by using the arguments of the previous section to say that the neutrino to photon conversion approximately takes place at a definite time, which we call t_C. According to Equation (78) this would be the time corresponding to $z \approx 200$. Then

$$N_\gamma(t_{\mathrm{now}}) \approx N_\nu(t_C) \times C \times \left(\frac{a(t_C)}{a(t_{\mathrm{now}})}\right)^3. \tag{80}$$

The first factor is the number density of relevant neutrinos at t_C, C the conversion probability (Equation (69)), and the last factor is the dilution factor to the present.

6.3.1. $\mathrm{N}_\nu(\mathrm{t_C})$

By the density of relevant neutrinos we mean those of sufficient energy to produce positrons. We call this energy E_{th}.

Since the neutrinos are not significantly absorbed between t_{cmb} and t_C, we may refer the calculation to our reference point t_{cmb} and perform the necessary redshift to t_C. One thus obtains

$$N_\nu(t_C) = \int_{5E_{\mathrm{th}}}^{\infty} \frac{dN_\nu(t_{\mathrm{cmb}})}{dE^\nu_{\mathrm{cmb}}} dE^\nu_{\mathrm{cmb}} \times \left(\frac{a(t_{\mathrm{cmb}})}{a(t_C)}\right)^3. \tag{81}$$

The factor of 5 in the lower limit of integration results from the fact that the redshift at t_C is about one-fifth that at our reference point t_{cmb}. Inserting in Equation (80):

$$N_\gamma(t_{\mathrm{now}}) \approx \int_{5E_{\mathrm{th}}}^{\infty} \frac{dN_\nu(t_{\mathrm{cmb}})}{dE^\nu_{\mathrm{cmb}}} dE^\nu_{\mathrm{cmb}} \times C \times \left(\frac{a(t_{\mathrm{cmb}})}{a(t_{\mathrm{now}})}\right)^3. \tag{82}$$

The cancellation of the $a(t_C)$ factor reflects the fact the neutrino and photon densities redshift in the same way. The cancellation shows that in a more detailed treatment where one performs an average over conversion times t_C, the only significant difference will be in the resulting average over E.

Using $C \approx (5 \times 10^{-14})\,(E^\nu/\mathrm{GeV})$ and the redshift of 10^{-3} for t_{cmb}, Equation (82) becomes finally

$$N_\gamma(t_{\mathrm{now}}) \approx (5 \times 10^{-23})\,(E^\nu/\mathrm{GeV}) \times \int_{5E_{\mathrm{th}}}^{\infty} \frac{dN_\nu(t_{\mathrm{cmb}})}{dE^\nu_{\mathrm{cmb}}} dE^\nu_{\mathrm{cmb}}. \tag{83}$$

Naturally if the neutrino spectrum does not extend above threshold, which we will be here taking as 5 MeV at t_{cmb}, all such integrals should be set to zero.

6.3.2. Model with $\bar{E}^\nu$

For general orientation we evaluate Equation (83) in some of the schematic models. In the model with a well-defined emission energy, we use Equation (50) and integrate from 5 MeV to infinity, finding (with $x_{\mathrm{min}} \ll 1$)

$$N_\gamma(t_{\mathrm{now}}) \approx \frac{(6 \times 10^{15})}{\mathrm{s}^3} \frac{M_{\mathrm{pl}}}{5\ \mathrm{MeV}} (5 \times 10^{-23})\,(E^\nu/\mathrm{GeV})\mathcal{P} = \frac{(0.7 \times 10^{15})}{\mathrm{s}^3} (E^\nu/\mathrm{GeV})\mathcal{P} \quad E^\nu \gg 5\,\mathrm{MeV}, \tag{84}$$

Thus a 10 m on a side square detector would have a rate $\sim 0.7 \times (E^\nu/\mathrm{GeV})\mathcal{P}\,\mathrm{s}^{-1}$. While much depends of course on the values of $\mathcal{P}$ and E^ν, this seems a nontrivial result. We stress that this formula results from taking $\mathcal{P}$ constant, otherwise it should be understood as some weighted average of $\mathcal{P}$ over emission times x, according to the earlier formulas.

6.3.3. Spread Spectrum Model

From the discussion in Section 5.2.2, there are two different formulas to evaluate, according to whether the curve for a given E^ν_{cmb} in Figure 1 is first stopped by the "escape" line or by the E_{max} line.

6.3.4. $E_{\max} \gtrsim 10^{15}$ GeV

For a high enough $E_{\max}$, above about 10^{15} GeV, but still below the Planck scale, all neutrino pulses have components which are stopped by the escape condition, and so the second option in Equation (62) should be used for all energies $E^{\nu}_{\rm cmb}$.

Dividing by E for the number density we then need the expression

$$\begin{aligned}\int_{5E_{\rm th}}^{\infty} \frac{dN_{\nu}(t_{\rm cmb})}{dE^{\nu}_{\rm cmb}} dE^{\nu}_{\rm cmb} &= \frac{(6\times 10^{15})}{s^3}\frac{M_{\rm pl}}{E_{\max}}\mathcal{P} \\ &\times \int_{5\ {\rm MeV}}^{\infty}((s\times E^{\nu}_{\rm cmb}/{\rm GeV})^{-1/3}-1)\frac{1}{E^{\nu}_{\rm cmb}}dE^{\nu}_{\rm cmb} \\ &\approx \frac{(6\times 10^{15})}{{\rm s}^3}\frac{M_{\rm pl}}{E_{\max}}\mathcal{P}\times 3(s\times 5\ {\rm MeV}/{\rm GeV})^{-1/3} \\ &= \frac{(4\times 10^{21})}{{\rm s}^3}\frac{M_{\rm pl}}{E_{\max}}\mathcal{P}, \end{aligned} \tag{85}$$

and so for Equation (83):

$$\begin{aligned} N_{\gamma}(t_{\rm now}) &\approx \frac{(5\times 10^{-23})}{{\rm s}^3}(E^{\nu}/{\rm GeV}) \\ &\times (4\times 10^{21})\frac{M_{\rm pl}}{E_{\max}}\mathcal{P} \\ &= \frac{(2\times 10^{-1})}{{\rm s}^3}(E^{\nu}/{\rm GeV})\frac{M_{\rm pl}}{E_{\max}}\mathcal{P} \\ &= \frac{(2\times 10^{18})}{{\rm s}^3}\frac{E^{\nu}}{E_{\max}}\mathcal{P}. \end{aligned} \tag{86}$$

With $E_{\max}$ so large and E^{ν} in the MeV or GeV range, this will be very small in comparison with Equation (84), reflecting the fact that only a small fraction of the neutrino pulse "escapes."

6.3.5. $E_{\max} \lesssim 10^{15}$ GeV

We now come to the case of the spread spectrum where $E_{\max}$ is low enough that most neutrinos escape, using the first option of Equation (62), so that one has

$$\int_{5E_{\rm th}}^{\infty} \frac{dN_{\nu}(t_{\rm cmb})}{dE^{\nu}_{\rm cmb}} dE^{\nu}_{\rm cmb} = \frac{(6\times 10^{15})}{{\rm s}^3}\frac{M_{\rm pl}}{5\ {\rm MeV}}\mathcal{P}. \tag{87}$$

which is the same as in the first line of Equation (84), leading to the same conclusions.

6.3.6. Emission Times

Since a certain neutrino energy is required for the positron production, there are limitations on how early the neutrinos can originate. In Figure 1, the descending curves indicate those times for which a certain neutrino energy appearing at $t_{\rm cmb}$ can be emitted. Where such curves enter the forbidden zone below the ascending straight line, the neutrinos can no longer "escape." This earliest time is given by the scaled time $x = (sE_{\rm cmb}/{\rm GeV})^{2/3}$. If we set $E_{\rm cmb} = 5$ MeV in order to have 1 MeV at $z \approx 200$, this gives an earliest emission time of about 5×10^2 s. If we set $E_{\rm cmb} = 5$ GeV in order to have a larger cross section for the positron production, then the earliest time becomes about 5×10^4 s. Hence a positron signal would indicate burst activity around these times or later.

6.4. Reionizations by 511 keV Photons

A flux of 511 keV photons after recombination will lead to some reionizations of the newly formed hydrogen atoms. Even though these photons may not "escape" to us, there is the question if these reionizations might be significant.

To examine this possibility we consider a certain density $N_{\gamma}(t_{\rm cmb})$ of the 511 keV photons at $t_{\rm cmb}$ and ask for the probability for an hydrogen atom to be subsequently ionized. The probability ${\rm Prob}_{\rm ioz}$ of an atom being ionized per unit time dt is

$$\frac{d\ {\rm Prob}_{\rm ioz}}{dt} = N_{\gamma}(t)\ M\times \sigma_{\rm ioz}, \tag{88}$$

where $\sigma_{\rm ioz}$ is the cross section for the ionization of an atom by a 511 keV photon. M is a factor to account for the multiple ionizations that can be induced by a high-energy photon.

The density of the photons will decrease with time as $N_{\gamma}(t_{\rm cmb})(a(t_{\rm cmb})/a(t))^3 = N_{\gamma}(t_{\rm cmb})(t_{\rm cmb}/t)^2$ so that one has for the integrated probability for an atom to be ionized:

$$\begin{aligned}{\rm Prob}_{\rm ioz} &\approx N_{\gamma}(t_{\rm cmb})M\sigma_{\rm ioz}\int_{t_{\rm cmb}}^{\infty}(t_{\rm cmb}/t)^2 dt \\ &= N_{\gamma}(t_{\rm cmb})M\times\sigma_{\rm ioz}\times t_{\rm cmb}. \end{aligned} \tag{89}$$

In principle $\sigma_{\rm ioz}$ is also a function of time due to the redshift of the photons, but the integral is dominated by times close to $t_{\rm cmb}$, so we may take it as constant.

Around 500 keV the cross section of photons on hydrogen is (2.8×10^{-25}) cm^2, see Equation (73). Attributing this all to ionization, one has then for the approximate probability for an atom to be ionized

$$\begin{aligned}{\rm Prob}_{\rm ioz} &\approx N_{\gamma}(t_{\rm cmb})M\times(2.8\times 10^{-25}\ {\rm cm}^2) \\ &\times(9\times 10^{12}\ {\rm s}) \\ &= (7\times 10^{-2})\,N_{\gamma}(t_{\rm cmb})M\ {\rm cm}^3 \\ &= (3\times 10^{-33})\,N_{\gamma}(t_{\rm cmb})M\ {\rm s}^3. \end{aligned} \tag{90}$$

Thus the density $N_{\gamma}(t_{\rm cmb})$ would have to be very large to have a significant effect on recombination. For example, if we take the estimate Equation (84) multiplied by 10^9 to refer to $t_{\rm cmb}$, with 1 GeV neutrinos and $M = (5\times 10^4)$, as would correspond to converting essentially all the energy of an absorbed photon into ionization, one finds that the probability of an atom being ionized is $\sim 10^{-4}\ \mathcal{P}$.

Although this estimate will vary according to the form of $\mathcal{P}$, it appears that the reionizations are not significant. However, should it come to pass that the positron mechanism turns out to be much stronger than in our simple estimates, then this reionization could lead to small ionized patches after recombination, which would be a way of seeing the "escaping" neutrinos directly. Also, in this case of very strong neutrino pulses, it might be interesting to consider $\nu + H \rightarrow \nu + e^- + p$ as a source of ionizations. Patchy reionization could be a target for next generation ground-based 21 cm and CMB experiments, which should be capable of detecting it. These include improvements to HERA, which probes the 21 cm power spectrum to $z \approx 8$ (P. M. Keller et al. 2023), and EDGES (R. A. Monsalve et al. 2017), SARAS-3 (H. T. J. Bevins et al. 2022), and NenuFAR (S. Munshi et al. 2024), which set limits on H I nondetection at $z \sim 20$.

6.5. Conclusions on Positrons

The above results suggest that when energies of the neutrinos in a pulse are low enough so that most of them "escape," but high enough to produce positrons, then Equation (84) will apply, which for $\mathcal{P}$ not too small, can lead to a potentially observable signal of $\sim$2 or 3 keV X-rays at present. In this energy range, the soft X-ray sky is dominated by local emission. Observed fluxes are from diffuse gas in the local hot bubble, the Milky Way diffuse hot gas (M. Ueda et al. 2022), and even circumgalactic hot gas (G. Ponti et al. 2023). However it is possible that the characteristic form of the "bump" in the spectrum could allow it to be picked out among these broad backgrounds.

7. "Contained" Bursts, the "Heat Signal"

The bursts are a nonequilibrium phenomenon, quite different from the stages of quasi-thermal equilibrium assumed in the standard cosmology, and it is by this aspect that we hope to identify them.

Above we considered manifestations of burst particles that "escape." We now consider bursts that are "contained," where the particles interact before $t_{\rm cmb}$. In particular we examine the possibility of nevertheless obtaining a signal from their energy deposit. If the volume occupied by the "contained"burst is relatively small, it is possible that the deposited energy leaves a significant signal. We call this the "heat signal."

The features of the heat signal, for our purposes, are essentially determined by the light cones of the general relativistic kinematics and not so much by any particular properties of the medium or the particles. This is perhaps in contrast to the more familiar studies of diffuse energy injection in the more local Universe (W. Hu & J. Silk 1993).

For the "contained" bursts, there are two general mechanisms for the spread of the burst energy from very early times. One is from the essentially free flight of the neutrinos before they interact. The second is a diffusion of the energy, mostly carried by the electromagnetic and strong interaction components, after the neutrinos interact and convert. Since diffusion is a multiple scattering process, one might expect the first mechanism to usually dominate. In this case, when the "free flight" determines the expected dimension, the heated region will be simply "frozen in" at the free flight distance. However under certain conditions it may be that the diffusion distance becomes significant. Below, we attempt a crude estimate as to when this may occur.

There is a large body of later work, most notably the papers on detailed modeling of energy transfer, pioneered by J. Chluba and colleagues, ranging from generic early energy injection (S. K. Acharya & J. Chluba 2022; S. K. Acharya et al. 2024), to hydrogen and helium recombination lines (L. Hart et al. 2020), and synergy with CMB anisotropies (M. Lucca et al. 2020). The observational situation remains unsatisfactory with no progress on spectral distortion limits since the COBE-FIRAS experiment. The expectation is that only the implementation of ESA's VOYAGE2050 road map will enable a definitive CMB spectral distortion mission, that will improve on FIRAS by some 5 orders of magnitude in sensitivity to the μ spectral distortion.[7] However even here the possible achievable angular resolution may be inadequate to probe the CMB parameter space of hot spots that we seek to explore.

We stress that here we are concerned with direct heating of small regions soon after the thermalization of the CMB.

We provide some approximate, intuitive arguments for the relevant quantities. These could in principle be obtained from global treatments, such as the state-of-the-art Einstein–Boltzmann public codes CLASS and CAMB, which incorporate the full physics of diffusion damping.

Given a burst originating at some spacetime coordinates (t, x), the energy in freely flying neutrinos will spread from this point along the light cone. After the neutrinos have been stopped, the energy will propagate much more slowly, filling in the light cones. When this further propagation is relatively small the energy is essentially contained within the "free flight" distance. As was explained above, this distance is governed by $t_{\rm free}$. When the diffusive distance is greater, the distance is governed by a dimension as in Equation (23). The contained bursts are represented by the small circles in Figure 2.

Examples for complete "containment" of the bursts may be seen in Table 1 for those entries where $\mathrm{Prob}_\infty \approx 0$. In Figure 1 this corresponds to neutrinos emitted below the $x = sE$ line. These figures are for neutrinos and are based on an estimate using weak interaction parameters. Other carriers of the propagating energy involving electromagnetic or strong interactions, will have a much more localized containment of the energy. However, when the neutrinos carry nearly all the energy, analogous to the case of core-collapse supernovae, then Table 1 may taken to apply realistically. There is nevertheless the possibility that some particles of a burst are "contained" while others are not, as in the spread spectrum model.

The signal would then arise on certain small angular scales on the CMB, and this morphology would be characteristic for the "contained" bursts. The linear dimension at the CMB corresponding to "free flight" from $t_{\rm em}$ to $t_{\rm cmb}$ was given in Equation (18) as

$$2t_{\rm cmb}^{1/2}(t_{\rm free}^{1/2} - t_{\rm em}^{1/2}) = 2t_{\rm cmb}(x_{\rm free}^{1/2} - x_{\rm em}^{1/2}), \tag{91}$$

using the scaled time x in the second writing. A signal would be on angular scales corresponding to this proper size on the CMB. The dimensional parameter in Equation (91) is $t_{\rm cmb}$, which expressed as a conventional length is about 10^4 Mpc. This is the largest size a "burst spot" could be (on the CMB) and gets smaller as $x_{\rm em} \to x_{\rm free}$, until the burst "escapes."

We recall that Equation (91) was found by using the dimensions of the region in which a neutrino pulse is absorbed, which is why $t_{\rm free}$ appears. This implies the assumption that there is no important further spread of the energy after the neutrinos have been stopped, which seems plausible in view of the small value of the diffusion distance (Equation (23)).

However, this assumption could be wrong if a significant portion of the burst is transferred to a propagating form of energy such as acoustic waves. Equation (91) would approximately also apply to the propagation of sound waves, since these are expected to travel at close to the speed of light in the relativistic plasma, with $t_{\rm free}$ replaced by a damping distance. The dimensional parameter and so the size of the "spot" should remain essentially the same.

This damping was studied extensively in the work on early energy injection mentioned above. For our considerations, we

[7] https://www.cosmos.esa.int/documents/1866264/1866292/Voyage2050-Senior-Committee-report-public.pdf

note that according to J. Chluba et al. (2012) for example, density perturbations in regions smaller than about .02 Mpc $= (2 \times 10^4)$ pc will be damped out (by photon diffusion) by the time of the formation of the CMB. The wavelength of possible sound waves induced by the bursts might be expected, at most, to be the size of the burst region at emission, after redshift to $t_{\rm cmb}$. This quantity is $9 \times 10^9\,(t_{\rm em}/{\rm s})^{1/2}$ s. Since for the dimensional factor here we have 9×10^9 s $= 90$ pc, it appears that the part of the burst energy appearing as density perturbations from sonic waves will have been degraded by $t_{\rm cmb}$ and thus can also contribute to a "heat signal."

While we imagine that the energy of a neutrino pulse will be dissipated mainly by a diffusion-like process as in cosmic-ray showers (T. K. Gaisser et al. 2016), the subject of possible acoustic waves seems an interesting one in further studies.

7.1. Estimate of the Effect of "Contained" Energy

After the question of the size of a possible "hot spot," the remaining question is the magnitude of the possible heating.

It is possible to make an estimate of the possible significance of this "heat signal" without a detailed description of the thermalization process as developed in J. Chluba et al. (2012).

Our argument is as follows.

We gauge the significance of this energy deposit from a burst by estimating what temperature rise ΔT it would produce, given the heat capacity C of the region of "containment." If this ΔT turns out to be not very small compared to the temperature at $t_{\rm cmb}$, it suggests a potentially observable effect. This is a conservative estimate, since the use of the thermal heat capacity assumes the deposited energy has been spread over all degrees of freedom uniformly, while it is possible that the energy does not have time to completely thermalize.

7.1.1. "Free Flight" Region

We first consider the heating of a region whose volume is determined by the length in Equation (91). One needs the burst energy, after the redshift to $t_{\rm cmb}$. From our assumption that the energy of a burst at emission is the energy in a horizon volume or energy density $\times$ volume, we write

$$E^{\rm burst}_{t_{\rm cmb}} = U_{\rm em} V_{\rm em} \frac{a(t_{\rm em})}{a(t_{\rm cmb})}, \tag{92}$$

with $U_{\rm em}$ the energy density at emission and $V_{\rm em}$ the horizon volume at emission. We find the ΔT induced by this energy from the heat capacity at $t_{\rm cmb}$. In terms of C_V, the heat capacity per unit volume, we have at $t_{\rm cmb}$

$$C = C_V \times V_{\rm cmb} = \frac{4 U_{\rm cmb}}{T_{\rm cmb}} \times V_{\rm cmb}, \tag{93}$$

where in the second step we use the relation between C_V and U for a relativistic gas, $C_V = 4\,U/T$. $V_{\rm cmb}$ is the volume occupied by the burst at $t_{\rm cmb}$. Taking the ratio of Equation (92) to Equation (93) and dividing by $t_{\rm cmb}$ we find at $t_{\rm cmb}$

$$\frac{\Delta T}{T} = \frac{1}{4} \frac{U_{\rm em}}{U_{\rm cmb}} \frac{a(t_{\rm em})}{a(t_{\rm cmb})} \frac{V_{\rm em}}{V_{\rm cmb}}. \tag{94}$$

The ratio of the energy densities is as $(T_{\rm em}/T_{\rm cmb})^4$ or $(a(t_{\rm cmb})/a(t_{\rm em}))^{-4}$ so Equation (94) is

$$\frac{\Delta T}{T} = \frac{1}{4} \left(\frac{a(t_{\rm cmb})}{a(t_{\rm em})} \right)^3 \frac{V_{\rm em}}{V_{\rm cmb}}. \tag{95}$$

The ratio of volumes goes as the cube of the linear dimensions. At $t_{\rm em}$ the linear dimension is the horizon or 2 $t_{\rm em}$, and for the burst at $t_{\rm cmb}$ we have from Equation (18) the linear dimension approximately $2 t_{\rm cmb}^{1/2} t_{\rm free}^{1/2}$ Inserting the cubes in Equation (95):

$$\begin{aligned} \frac{\Delta T}{T} &= \frac{1}{4} \left(\frac{a(t_{\rm cmb})}{a(t_{\rm em})} \right)^3 \left(\frac{t_{\rm em}}{(t_{\rm cmb} t_{\rm free})^{1/2}} \right)^3 \\ &= \frac{1}{4} \left(\frac{t_{\rm em}}{t_{\rm free}} \right)^{3/2} = \frac{1}{4}\, \kappa^{-3/2}, \end{aligned} \tag{96}$$

using $a \sim t^{1/2}$. (If one does not wish to make the approximation $t_{\rm em}/t_{\rm free} \ll 1$ in the linear dimension then there is an additional factor of $(1 - t_{\rm em}^{1/2}/t_{\rm free}^{1/2})^{-3}$.)

We are considering the "contained" case so $\kappa = t_{\rm free}/{\rm t_{em}}$ is greater than one. But for bursts that are "well contained," where κ is not very much larger than one, it thus appears that an interesting degree of "heating" is possible. This signal would be visible as a deviation from a Planckian spectrum in regions of sizes given in Equations (18) or (23) if the energy has not had time to thermalize. Or if the energy is thermalized, as a simple temperature fluctuation, it would be necessary to disentangle this from other sources of temperature fluctuations. Understanding whether essentially complete thermalization occurs or not would require a detailed analysis going beyond our simple one-component model of the plasma. But the non-Planckian spectrum, which of course is a nonequilibrium feature, would be characteristic for the bursts.

7.1.2. "Diffusive" Region

The above estimate for the heat signal was based on using the "free flight" estimate for the size of the heated region at $t_{\rm cmb}$. We can do the same for the opposite case, for the small "diffusive" region, using the estimate Equation (23) for the size of the region.

Since we argued that the dimensions of the "diffusive" region are constant, independent of the emission time, the only variable in the problem is the energy of the burst. As expressed in Equation (27) in terms of the scaled emission time x this is $E^{\rm tot}_{\rm cmb} = (2 \times 10^{56})\ x^{3/2}\, M_{\rm pl}$

One then finds

$$\begin{aligned} \frac{\Delta T}{T} &\sim \frac{(2 \times 10^{56})\ x^{3/2}\, M_{\rm pl}}{T^4 d^3 {\rm lt{-}yr}^3} \approx (7 \times 10^{18})\, \frac{x^{3/2}}{d^3} \\ &= 0.3\ (t_{\rm em}/\ {\rm s})^{3/2} \frac{1}{d^3}. \end{aligned} \tag{97}$$

The quantity d is the linear dimension of the potentially heated region in light years. T is the temperature at $t_{\rm cmb}$.

If other propagating modes such as sound waves are important in the energy spread, then one may expect an effect in between the two extremes we have examined here: for a large "ballistic region" and a small "diffusive region."

Finally, we note we have been assuming that the full energy of the burst is "contained." However, for bursts that are not very early, or which contain a wide spread of particle energies,

this may not be the case. For example, in the simple spread-out model of Section 5.2.2, Equation (54), the fraction of the energy "escaping" is $(x_{\rm em}/{\rm s})({\rm GeV}/E_{\rm max}) = 1 \times (t_{\rm em}/\ {\rm s})({\rm GeV}/E_{\rm max})$. In such cases the $\Delta T/T$ value must be reduced according to the fraction not escaping. However for high particle energies or early emission times the escape fraction goes to zero and all the energy is "contained."

8. Many Small Bursts

In the previous section, we studied the heat signal from a distinct single burst. As we go back in time, to ever smaller x, although the burst gets weaker, $\sim x^{3/2}$, the great increase in the number of potential emitting regions may compensate for the decreasing intensity. If the bursts do in fact arise from transitions to new spacetime regions, it is plausible that the underlying quantum tunneling proceeds with higher probability for the smaller horizon-sized regions at early times as $x \to 0$.

In this section, we thus speculate on the possibility of many small overlapping burst regions. We assume that all energies from a burst are "contained" and so the energy delivered to $t_{\rm cmb}$ from a single burst is Equation (27), namely $(2 \times 10^{56})\ x_{\rm em}^{3/2}\ M_{\rm pl}$.

8.1. Total Energy from Very Early Bursts

According to Equation (36), the energy density contribution from such many early time bursts would be the integral of $(3 \times 10^{15})\ \frac{M_{\rm pl}}{{\rm s}^3}\frac{\mathcal{P}(x)}{x}dx$. If $\mathcal{P}(0)$ does not vanish we expect a logarithmic divergence for the burst energy density

$$\epsilon_{\rm bursts}\ \sim (3 \times 10^{15})\ \frac{M_{\rm pl}}{{\rm s}^3} < \Delta\, x\mathcal{P}(0) > (-\ln x_{\rm min}), \qquad (98)$$

where $<\Delta x\mathcal{P}(0)>$ is some typical value of the integral $\int \mathcal{P}dx$ and $x_{\rm min}$ could correspond to the Planck time, $x_{\rm min} \sim 10^{-56}$.

Since we have many independent bursts from all directions, these would give a uniform background on the CMB. Taking the log to give 1 or 2 orders of magnitude, this suggest an energy density of bursts

$$\epsilon_{\rm bursts}\ \sim (10^{16}\ -\ 10^{17}\ ) < \Delta x\mathcal{P}(0) > \frac{M_{\rm pl}}{{\rm s}^3}. \qquad (99)$$

As remarked following Equation (47) with $\mathcal{P}(0)$ not too small this could be enough to give the total radiant energy density of the Universe. This is not surprising since we have assumed that the bursts are generated at the horizon scale. However we stress that a basic assumption in this paper is that $\mathcal{P}$ is so small that the usual cosmology is unaffected. It might be interesting to drop this assumption. This would invite a much wider discussion.

8.2. Fluctuations

Equation (98) represents simply a uniform average density, and so of itself is not obviously observable. However, what could be more characteristic for the picture are the associated statistical fluctuations. With many independent very early bursts of small energy one expects a statistical distribution of the burst energy over the patches of the sky under observation.

We consider the quantity $\overline{\delta E^2}$ or the variance characterizing the energy fluctuations from the bursts, whose square root is the typical energy fluctuation. Since we take the bursts to be independent statistical events a variance will result from the fluctuations in the number of events in the sample, as for a Poissonian or Gaussian distribution, where variance $\sim n$, where n is the average number of events. That is, we interpret the n in Equation (35) to refer to the average number of events, which then gives the variance. There could be further sources of variance such as fluctuations in the burst energy from a given epoch, but here we will simply take $\overline{\delta E^2} = \overline{\delta n^2}E^2 = nE^2$. For an interval of scaled cosmic time dx one has $n = \frac{dn}{dx}dx$

That is, the contribution from an interval of scaled cosmic time dx will be

$$\overline{(\delta E)^2}\ = \frac{dn}{dx}E^2(x)\,dx, \qquad (100)$$

where $E(t)$ is the energy in a single burst, Equation (27), namely $(2 \times 10^{56})x^{3/2}M_{\rm pl}$. We take $\frac{dn}{dx}$ from Equation (35) so that Equation (100) becomes

$$\begin{aligned}(\bar{\delta E})^2 &= V_{\rm obs} \times \frac{(2 \times 10^{-41})}{{\rm s}^3}\frac{\mathcal{P}(x)}{x^{5/2}}dx \\ &\quad \times ((2 \times 10^{56})\ x^{3/2}\ M_{\rm pl})^2 \\ &= \frac{V_{\rm obs}}{{\rm s}^3}(5 \times 10^{71})\ \mathcal{P}(x)\ x^{1/2}M_{\rm pl}^2 dx. \end{aligned} \qquad (101)$$

Adding up the contributions from all the dx intervals, one has for the integrated energy fluctuation itself then

$$\begin{aligned}((\bar{\delta E})^2)^{1/2} &= \left(\frac{V_{\rm obs}}{{\rm s}^3}\right)^{1/2}(7 \times 10^{35})\ M_{\rm pl} \\ &\quad \times \left(\int dx\ \mathcal{P}(x)\ x^{1/2}\right)^{1/2}. \end{aligned} \qquad (102)$$

An interesting aspect of this formula is that if $\mathcal{P}$ is a not too strongly increasing function for $x \to 0$, then the decreasing $x^{1/2}$ term could lead to a peak at some x, designating an epoch giving the greatest fluctuations.

Finally we have for the relative fluctuation of the burst energy at $t_{\rm cmb}$, using Equation (36), for the total burst energy density $\int (3.2 \times 10^{15})\ \frac{M_{\rm pl}}{{\rm s}^3}\frac{\mathcal{P}(x)}{x}dx$:

$$\begin{aligned}\frac{(\overline{(\delta E)^2})^{1/2}}{E} &= \left(\frac{V_{\rm obs}}{{\rm s}^3}\right)^{-1/2}(2 \times 10^{20}) \\ &\quad \times \frac{\left(\int \mathcal{P}(x)\ x^{1/2}dx\right)^{1/2}}{\int \frac{\mathcal{P}(x)}{x}dx}. \end{aligned} \qquad (103)$$

With the sort of values for $V_{\rm obs}$ mentioned after Equation (35), the prefactor here is relatively large, and could be made larger by observations with higher angular resolution. There is also the large value of $1/\sqrt{\mathcal{P}}$ implicit in the ratio factor with small $\mathcal{P}$. The observational aspect of many independent small fluctuations could thus be that the nonequilibrium "heat signal" features, discussed above for single bursts, become more pronounced for samples with higher angular resolution.

However since x is always less than one, these factors favoring large fluctuations will tend to be compensated by the small value for the ratio of the integrals. For example, with $\mathcal{P}(o)$ nonzero there is the behavior $x^{3/4}/\ln x$ for $x \to 0$, which would give a factor $\sim 10^{-44}$ toward the Planck time.

9. Time-dependent Phenomena

9.1. Intrinsic Burst Length

One of the most intriguing possibilities concerning the bursts would be the observation of an arriving burst. Much as we see the brightening of a star to a supernova, a small spot on the CMB might brighten and then fade. But unfortunately such an observation seems unlikely, as we discuss in this section.

In Equation (4) of J. Silk & L. Stodolsky (2006), we took the intrinsic length of a burst to be given by the size of the emitting region, using the horizon size. With the redshift to the present the length of a burst if it could be directly seen at the Earth would be

$$9 \times 10^9\,(t_{\rm em}/{\rm s})^{1/2}\ {\rm s} = (3 \times 10^{15})\, x_{\rm em}^{1/2}\ {\rm s}. \tag{104}$$

We note that this estimate of the timescale is based on using the horizon size as giving the natural dimensions. If there is a period of "neutrino trapping" (D. Z. Freedman et al. 1977) as in core-collapse supernovae, the timescale could be somewhat longer.

For early emission times, $t_{\rm em} \ll 1$ s, it thus seems conceivable that with an observation period of years the "arrival" of a burst could be seen, in principle. However, even if there were particles that would "escape" from such early times, their very great redshift would make them undetectable, at least as pulses. We thus consider our indirect methods of detection on the CMB, where however a number of points concerning time dependence should be considered.

9.2. Movement of Our Backward Light Cone

A preliminary question regarding time dependence concerns the movement of our BLC, i.e., an increase in the radius of the large circle in Figure 2. After a sufficiently long time, an observation in any given direction will be looking at a different patch at $t_{\rm cmb}$, with a different burst history. However, the time spread or averaging for a given observational arrangement is $d_{\rm thom}$, or several thousand years (Equation (33)). On the other hand at $t_{\rm cmb}$, the BLC moves out $a(t_{\rm cmb}) \times 1$ lt-yr in a year, or 10^{-3} lt-yr in 1 Earth year. Therefore, on the scale of years for an observation, one is always effectively viewing the same region of the CMB, and there should be little change in the phenomena originating from the bursts. (But it might be worth good record keeping of present observations for the use of colleagues in a distant future.)

9.3. Delay Due to Signal Production

An issue is the time delay connected with the production of the observable signal. The production of the signal can involve some time, and we consider this for the two mechanisms, the "positron signal" and the "heat signal."

9.3.1. Positron Mechanism

Here an essential element in the time structure will be the time it takes for a positron to annihilate after it is produced. At the low density of electrons around $t_{\rm cmb}$ or later, the positrons will wander for a considerable time before annihilating. We may roughly expect this to be on the same order as that determined by $d_{\rm thom}$ or several thousand light years. The lifetime for positrons in ordinary materials is $\sim 10^{-10}$ s. Rescaling for the density of electrons at $t_{\rm cmb}$ one finds $\sim 10^{11}$ s. Thus for observations made on the scale of years, any initial time structure for the positron signal will be washed out, even not accounting for the redshift to Earth time.

9.3.2. Heat Signal

We consider the simple cases of a fully contained burst, symbolized by the smallest circles in Figure 2. The small circles are to be imagined in or on the finite thickness of the large circle. The heat signal arises in the region in which the burst was absorbed, given essentially by $t_{\rm free}$. According to Section 3.2 the largest size of this region at $t_{\rm cmb}$ is given approximately by

$$\text{size}_{\rm cmb} \approx 2 t_{\rm cmb}^{1/2} t_{\rm free}^{1/2}, \tag{105}$$

which can vary greatly, according to the value of $t_{\rm free}$.

Generally, there are two possible sources of a time dependence of the signal. One is from changes in the nature of the "spot" itself during an observation period. The second could be alterations in the "observability," due to the motion of the large circle in Figure 2 during the observation time. Over a long enough period of time, a "spot" which is observable could move on or off the big circle. However, both types of effects should be small, not least because of the redshift of the observation time at Earth to $t_{\rm cmb}$. We characterize the length of an observation period in terms of $\Delta t_{\rm obs}$ Earth years, which corresponds to $(1 \times 10^{-3})\Delta t_{\rm obs}$ years at $t_{\rm cmb}$.

As an example of the first type of time dependence we consider the size of the burst region. Due to the expansion, the "spot" is growing during the observation. Other effects of this type might be shifts in the spectrum under study, but this must await a detailed study of the thermalization process.

To estimate the change in size, we use Equation (105) taken as a function of $t_{\rm cmb}$. Up until now, we have treated $t_{\rm cmb}$ as a constant, but this factor in Equation (105) arose from the expansion factor $a(t_{\rm cmb})$, and the expansion continues during the observation period. We then find for the relative size change

$$\frac{\Delta \text{size}_{\rm cmb}}{\text{size}_{\rm cmb}} = \frac{1}{2}\,\frac{\Delta t_{\rm cmb}}{t_{\rm cmb}} = \frac{1}{2}\,(1 \times 10^{-3})\,\frac{\Delta t_{\rm obs}}{t_{\rm cmb}}. \tag{106}$$

Since $t_{\rm cmb} \sim (4 \times 10^5)$ yr one sees that an observation this type, with years duration, will have to contend with the small factor $\sim 10^{-8}$.

Coming to the second type of effect, due to the movement of our BLC, the small parameter is the movement. In a $\Delta t_{\rm obs}$ of 1 Earth year, the radius of the large circle in Figure 2 increases by $a(t_{\rm cmb})\Delta t_{\rm obs} \approx 10^{-3}$ yr. For example, if a small burst is near the outer edge of the observation band, in 1 year it will move $\sim 10^{-3}$ yr closer to the center, brightening slightly. This is to be compared with the width of the observation band, symbolized by the thickness of the big circle. This dimension is given by $d_{\rm thom}$ or several thousand years. The ratio then is also small, $\sim 10^{-7}$. It would seem that such effects would be strongest when the size given by Equation (105) is about the same of the width of the band. Otherwise for small sizes the time variation will be controlled by the variation of the observability of the signal under consideration across the band, involving a detailed analysis.

A important practical consideration here is likely to be if the sought-for deviations from the thermal spectrum are detectable within the relatively short observation times. From Equation (104),

it seems that bursts that somehow could be detected directly at the Earth might have a reasonable length in time. However, we conclude here that those observed via the CMB may be regarded as permanently fixed on the sky, up to the very difficult measurements just described.

10. Assumptions, Approximations, and Further Work

In this section we note some of our most important assumptions and approximations, with the implied suggestions for further work.

Our most salient assumption is that the presently standard cosmology, with its parameters, may be used in the presence of the bursts. This seems a quite plausible assumption when $\mathcal{P}$, the burst probability, is very small. But how large a $\mathcal{P}$ is permitted within this assumption is a complex question. One simple estimate for its validity would follow from requiring that the burst energy transmitted to some relatively recent times, say $t_{\rm cmb}$, be much less the known energy at that time. According to Equation (36) the burst energy density at $t_{\rm cmb}$ is the integral of $(3 \times 10^{15})\ \frac{M_{\rm pl}}{s^3}\frac{\mathcal{P}(x)}{x}dx$. With the standard energy density $(\pi^2/15)T^4 = (8 \times 10^{35})$ GeV s^{-3} at $t_{\rm cmb}$, this leads to the amusingly simple condition

$$\int_0^1 \mathcal{P}(x)\frac{dx}{x} \ll 1. \tag{107}$$

While it seems evident that Equation (107) is a necessary condition that the standard cosmology is not significantly affected, an interesting subject for further study is if it is also a sufficient condition.

A further assumption was that in writing the simple Equation (25) for the redshift of the total energy of a burst we have assumed that the redshift is radiation-like, even for the secondary reaction products in the medium. This assumption might have to be reexamined in situations where a significant portion of the energy ends up being carried by nonrelativistic components.

On a more technical level, one of our simplifying assumptions is the use of the radiation-dominated epoch formula $a \sim t^{1/2}$ all the way to $t_{\rm cmb}$, while strictly speaking it should only be used until the somewhat earlier time of radiation–matter equality $t_{\rm eq}$. This however does not lead to a very large error in the numerical estimates; the value of $a(t_{\rm cmb})$ this way is 0.7×10^{-3} instead of the more correct 1.0×10^{-3}, and it permits much more transparent formulas, and identification of the essential issues.

10.1. Neutrino Absorption Parameters

The use of only 1 degree of freedom for the ambient medium and a generic neutrino cross section to find the neutrino absorption, allows us a simple identification of the main features of our problem. A more exact treatment would take into account the increase in the number of degrees of freedom with energy and particular features affecting the cross section such as nucleosynthesis or phase transitions. While the general features we have found should remain, alterations in the numerical factors may be expected.

10.2. "New Physics"

A further assumption was our use of arguments and parameters based on a simple extrapolation of presently known information, while there is the possibility of "new physics" at yet higher energies than have been explored to date.

The most likely of these possibilities concerns our Equation (1), which controls our estimates of neutrino absorption. This formula represents lowest-order perturbation theory for weak interactions, which gives the cross section increasing with the center-of-mass energy squared S. It is not plausible that this increase continues indefinitely at very high energy. Once the cross section reaches a value corresponding to the geometric range of the interaction, unitarity arguments suggest that the growth must saturate. The linear growth with S will probably then go over to the much slower $(\ln S)^2$ growth, as is known for strong interactions (L. Stodolsky 2017). This geometric range of the weak interactions is given by the exchange of W and Z vector bosons, that is, by our $M = 100$ GeV parameter via range $= 1/M$. We thus anticipate that our estimates are approximately valid until energies where

$$\left(\frac{\alpha}{M^2}\right)^2 S \approx \pi\left(\frac{1}{M}\right)^2, \tag{108}$$

or until the center-of-mass energy squared

$$S = \frac{\pi}{\alpha^2}M^2 \approx (6 \times 10^8)\ \text{GeV}^2. \tag{109}$$

In terms of the interaction of our burst particles of energy $E_{\rm em}$ with the ambient plasma at temperature T this means that our considerations are valid up to values of $E_{\rm em} \times T$ given by $E_{\rm em}T = E_{\rm em}(2.5 \times 10^{-4})$ eV$/a \approx (6 \times 10^8)$ GeV^2. (For the kinematics see the discussion following Equation (1).)

Using $a = (t/t_{\rm rad})^{1/2}$ this implies that our simple discussions apply when

$$E_{\rm em} < (t_{\rm em}/\ \text{s})^{1/2}(5 \times 10^{11})\ \text{GeV}. \tag{110}$$

This constraint will only be relevant for the highest energies; the values in Table 1 are unaffected, for example. But it could play a role toward the Planck scale $\sim 10^{19}$ GeV, if we wish to speculate about that regime.

One may rearrange Equation (110) in terms of the scaled time x to give the condition

$$x > 10^{-36}\,(E_{\rm em}/\text{GeV})^2. \tag{111}$$

On Figure 1 the boundary of this region would be a quadratically increasing curve with very small coefficient. It finally crosses the linearly increasing "escape" boundary, but only at very high energy, near the Planck scale. This implies that our treatment remains qualitatively correct for essentially the entire region of the $E_{\rm em}$–x plane, except for Planck scale energies at late times.

10.3. Calculation of $\mathcal{P}$

The most important open question in our presentation lies in the production of the bursts. With knowledge or models for $\mathcal{P}$, its size and time dependence, and of how the potentially visible energy of the burst is set free, our formulas could be evaluated in more detail. Particularly useful would be a knowledge of the particle energy spectrum, to avoid the very simplified model assumptions of Section 5.

It should also be noted that in addition to bursts originating from gravitational processes like the creation of "baby Universes" or supermassive black hole formation, it has been suggested that there could have been "little bangs," connected

with phase transitions in the very early Universe (C. P. Korthals Altes 1992). It is to be anticipated that these also will lead to the kind of signals we discuss. Further work here would be the adaptation of our parameters for these kinds of processes.

10.4. Gravitational Waves

An important associated question would be the production of gravitational waves, which might then be an observable signal for the bursts. The recent discovery of a stochastic gravitational-wave background (G. Agazie et al. 2023), first interpreted as a signature of the gradual inspirals preceding early supermassive black hole mergers, although such events rates may fall short by up to an order of magnitude (G. Sato-Polito & M. Zaldarriaga 2025), might be equally attributable to other physics (A. Afzal et al. 2023) that could include phenomena such as early bursts. It would be of great interest if the angular resolution of gravitational-wave detection allowed a directional identification with one of our "heat signals."

10.5. Burst Thermalization

A detailed description of the partial thermalization of the burst energy, particularly that of the neutrino pulse, would be valuable in connection with the appearance of the nonequilibrium "heat signal." Knowledge of the form of the deviation from the standard Planckian spectrum would be important. Due to the increase of the neutrino cross section with energy it is likely that this deviation appears as a high-energy component, but a detailed calculation would be useful. In addition to determining more accurately the diffusion length, such an analysis should also examine the free flight length, for a more detailed understanding of the heat signal.

An aspect of further work on this topic could be the study of collective mechanisms such as plasma oscillations and acoustic waves for the spread and dissipation of the burst energy (J. Chluba et al. 2012). These will of course involve much stronger interactions than for neutrinos and so smaller regions. But if they are important and do not dissipate, these would cause hot spots in the CMB and generate non-Gaussian features on small angular scales at the centers of the bursts. See for example statistical discussions of using such features to probe CMB non-Gaussianity (P. Chingangbam et al. 2012) and more recently by M. I. Khan & R. Saha (2022).

Finally, an important aspect of the "heat signal" which would be enabled by detailed modeling is the contribution of the bursts to the power spectrum of the CMB temperature fluctuations, in effect via a generalization of peak statistics in the cosmological context (J. M. Bardeen et al. 1986). Roughly speaking, the size of the contribution will be given by the magnitude of $\mathcal{P}$ and the angular scale will be governed by $t_{\rm free}$, or d. By comparison with existing or future data, limits on or values for these quantities could be estimated.

11. Conclusions

It is possible, and we feel likely, that major transformations of spacetime in the very early Universe led to peripheral phenomena, which we call "bursts" (J. Silk & L. Stodolsky 2006), which are potentially observable in our part of the Universe.

We have identified three possible signals of such bursts. One, and probably the most difficult observationally, would be a nonthermal addition to the low-energy neutrino spectrum anticipated for thermal relic neutrinos (Section 5.3). The two others would be effects conceivably accessible by present technologies or their extensions, namely small regions on the CMB with a nonthermal photon spectrum and, finally, the production of positrons leading to an ∼2 or 3 keV soft X-ray population (Section 6). While none of these signals seem easy to detect, their detection would would provide evidence for the most dramatic events in the history of the Universe and usher in a new era of observational cosmology.

Appendix
Units

In this paper we continue to use the simplest FRW cosmology as explained in the appendix of J. Silk & L. Stodolsky (2006), with the notation and parameters described there. However, the parameter $t_{\rm now}$, which appears in the late-time $a(t) = (t/t_{\rm now})^{2/3}$ should, in view of more recent data, be set to $t_{\rm now} \approx (2.9 \times 10^{17})$ s. To the one-place accuracy we are using, the other parameters remain unchanged, so we thus use $a = (t/t_{\rm rad})^{1/2}$ for early times with $t_{\rm rad} = 1.9 \times 10^{19}$ s. Also we use $a(t_{\rm cmb}) = 1.0 \times 10^{-3}$.

Additional parameters we use are $t_{\rm cmb} = (9 \times 10^{12})$ s so that $t_{\rm cmb}/t_{\rm rad} = (4.7 \times 10^{-7})$, and for the radius of our BLC at $t_{\rm cmb}$, $R_{\rm cmb}(blc) \approx (7 \times 10^{14})$ s. Also $T_{\rm now} = 2.9\,{\rm K} = (2.4 \times 10^{-4})$ eV and $T_{\rm now}^{-1} = (2.8 \times 10^{-12})$ s.

We generally use natural units ($\hbar = 1$, $c = 1$, and $k = 1$) and so express distances in light seconds or light years and temperature in eV units.

ORCID iDs

Joseph Silk https://orcid.org/0000-0002-1566-8148

References

Acharya, S. K., Cyr, B., & Chluba, J. 2024, MNRAS, 527, 9450
Afzal, A., Agazie, G., Anumarlapudi, A., et al. 2023, ApJ, 951, 11
Agazie, G., Anumarlapudi, A., Archibald, A. M., et al. 2023, ApJ, 951, 8
Acharya, S. K., & Chluba, J. 2022, MNRAS, 515, 5775
Acharya, S. K., Chluba, J., & Sarkar, A. 2023, in 16th Marcel Grossmann Meeting. On Recent Developments in Theoretical and Experimental General Relativity, Astrophysics, and Relativistic Field Theories., ed. R. Ruffini & G. Vereshchagin (Singapore: World Scientific), 1628
Bardeen, J. M., Bond, J. R., Kaiser, N., & Szalay, A. S. 1986, ApJ, 304, 15
Bevins, H. T. J., Fialkov, A., Acedo, E., et al. 2022, NatAs, 6, 1473
Carr, B. J., & Hawking, S. W. 1974, MNRAS, 168, 399
Chingangbam, P., Park, C., Yogendran, K. P., & van de Weygaert, R. 2012, ApJ, 755, 122
Chluba, J., Khatri, R., & Sunyaev, R. A. 2012, MNRAS, 425, 1129
Chluba, J., Abitbol, M. H., Aghanim, N., et al. 2021, ExA, 51, 1515
Dijkgraaf, R., Gopakumar, R., Ooguri, H., & Vafa, C. 2006, PhRvD, 73, 066002
Duda, G., Gelmini, G., & Nussinov, S. 2001, PhRvD, 64, 122001
Easther, R., Guth, A. H., & Masoumi, A. 2016, arXiv:1612.05224
Feeney, S. M., Johnson, M. C., Mortlock, D. J., & Pe, H. V. 2011, PhRvL, 107, 071301
Fixsen, D. J., Hinshaw, G., Bennett, C. L., & Mather, J. C. 1997, ApJ, 486, 623
Freedman, D. Z., Schramm, D.N., & Tubbs, D.L. 1977, ARNPS, 27, 167
Formaggio, J. A., & Zeller, G. P. 2012, RvMP, 84, 1307
Gaisser, T., & Halzen, F. 2014, ARNPS, 64, 101
Gaisser, T. K., Engel, R., & Resconi, E. 2016, Cosmic Rays and Particle Physics (Cambridge, UK: Cambridge Univ. Press)
González, N. M. 2023, ECRS, 27, 089
Guth, A. H. 2000, PhR, 333, 555
Hebecker, A., Mikhail, T., & Soler, P. 2018, FrASS, 5, 35
Hartle, J. B., & Hawking, S. W. 1983, PhRvD, 28, 2960
Hart, L., Rotti, A., & Chluba, J. 2020, MNRAS, 497, 4535
Hawking, S. W., & Laflamme, R. 1988, PhLB, 209, 39
Hollik, W. 2022, Quantum Field Theory and the Standard Model (Singapore: World Scientific)

Hu, W., & Silk, J. 1993, PhRvD, 48, 485
Keller, P. M., Nikolic, B., Thyagarajan, N., et al. 2023, MNRAS, 524, 583
Khan, M. I., & Saha, R. 2022, JCAP, 2022, 006
Kopp, M., Hofmann, S., & Weller, J. 2011, PhRvD, 83, 124025
Korthals Altes, C. P. 1992, in Gauge Theories, ed. R. Akhoury et al. (Singapore: World Scientific)
Kotera, K. 2021, ICRC (Berlin), 37, 1181
Landau, L. D., & Lifshitz, E. M. 1962, Classical Theoy of Fields (2nd ed.; Oxford: Pergamon Press), 280
Lucca, M., Schöneberg, N., Hooper, D. C., Lesgourgues, J., & Chluba, J. 2020, JCAP, 02, 026
Monsalve, R. A., Rogers, A. E. E., Bowman, J. D., & Mozdzen, T. J. 2017, ApJ, 847, 64
Munshi, S., Mertens, F. G., Koopmans, L. V. E., et al. 2024, A&A, 681, A62
Musco, I., De Luca, V., Franciolini, G., & Riotto, A. 2021, PhRvD, 103, 063538
Ponti, G., Zheng, X., Locatelli, N., et al. 2023, A&A, 674, A195
Rossi, N., Borghesi, A. A. M. G. B. M., Apponi, A., Betti, M. G., & Borghesi, M. 2024, in Proc. The European Physical Soc. Conf. on High Energy Physics (EPS-HEP2023) (Trieste: SISSA), 103
Silk, J., & Stodolsky, L. 2006, PhLB, 639, 14
Stodolsky, L. 1975, PhRvL, 34, 110
Stodolsky, L. 2000, PhLB, 473, 612000
Stodolsky, L. 2017, MPLA, 32, 1730028
Stodolsky, L., & Silk, J. 2025, PhRvD, 111, L121304
Sato-Polito, G., & Zaldarriaga, M. 2025, PhRvD, 111, 023043
The KM3NeT Collaboration, Aiello, S., Albert, A., et al. 2025, Natur, 638, 376
Ueda, M., Sugiyama, H., Kobayashi, B., et al. 2022, PASJ, 74, 1396
Vitagliano, E., Tamborra, I., & Raffelt, G. 2020, RvMP, 92, 045006
Weinberg, S. 1962, PhRv, 128, 1457
Weinberg, S. 1972, Gravitation and Cosmology by (New York: John Wiley and Sons)